Full characterization and transcript expression profiling of the interferon regulatory factor (IRF) gene family in Atlantic cod (*Gadus morhua*)

Authors: Sabrina M. Inkpen[1] (s.inkpen@mun.ca), Monica H. Solbakken[2] (m.h.solbakken@ibv.uio.no), Sissel Jentoft[2] (sissel.jentoft@ibv.uio.no), Khalil Eslamloo[1] (keslamloo@mun.ca), Matthew L. Rise[1*] (mrise@mun.ca)

[1]Department of Ocean Sciences, Memorial University of Newfoundland, NL, Canada, A1C 5S7

[2]Centre for Ecological and Evolutionary Synthesis (CEES), Department of Biosciences, University of Oslo, Oslo, Norway

*Corresponding author: Dr. Matthew L. Rise (email: mrise@mun.ca, phone: 709-864-7478)

Abstract

Atlantic cod (*Gadus morhua*) represents a unique immune system among teleost fish, making it a species of interest for immunological studies, and especially for investigating the evolutionary history of immune gene families. The interferon regulatory factor (IRF) gene family encodes transcription factors which function in the interferon pathway, but also in areas including leukocyte differentiation, cell growth, autoimmunity, and development. We previously characterized several IRF family members in Atlantic cod (*Irf4a, Irf4b, Irf7, Irf8*, and two *Irf10* splice variants) at the cDNA and putative amino acid levels, and in the current study we took advantage of the new and improved Atlantic cod genome assembly in combination with rapid amplification of cDNA ends (RACE) to characterize the remaining family members (i.e. *Irf3, Irf5, Irf6, Irf9,* and two *Irf2* splice variants). Real-time quantitative PCR (QPCR) was used to investigate constitutive expression of all IRF transcripts during embryonic development, suggesting several putative maternal transcripts, and potential stage-specific roles. QPCR studies also showed 11 of 13 transcripts were responsive to stimulation with poly(I:C), while 6 of 13 transcripts were responsive to lipopolysaccharide (LPS) in Atlantic cod head kidney macrophages, indicating roles for cod IRF family members in both antiviral and antibacterial responses. This study is the first to investigate expression of the complete IRF family in Atlantic cod, and suggests potential novel roles for several of these transcription factors within immunity as well as in early development of this species.

Keywords:

Atlantic cod, interferon regulatory factor, IRF, immune response, macrophage, development.

1. Introduction

The interferon (IFN) signalling pathway is a vital part of the vertebrate innate immune response to pathogens, and thus the study of genes involved in this complex process is important to our understanding of immune system function. Members of the interferon regulatory factor (IRF) family may either positively or negatively regulate the expression of IFNs and interferon stimulated genes (ISGs), playing an important role in the innate antiviral response (Honda and Taniguchi, 2006; Ozato *et al*., 2007). The IRF gene family may be divided into four sub-groups: IRF1-G (*Irf1*, *Irf2*), IRF3-G (*Irf3*, *Irf7*), IRF4-G (*Irf4*, *Irf8*, *Irf9*, *Irf10*), and IRF5-G (*Irf5*, *Irf6*) based on molecular phylogenetic analyses, reflecting expansion over evolutionary history and diversification of function (Nehyba *et al*., 2002; 2009). In most vertebrates studied, at least nine IRF genes (*Irf1*-*Irf9*) have been observed; a tenth family member (*Irf10*) is present in several avian and fish species, and another member of the IRF1-G sub-group (*Irf11* or *Irf1b*) has been identified in zebrafish (*Danio rerio*) and several other teleost fish (Stein *et al*., 2007; Huang *et al*., 2010; Huang *et al*., 2017). The presence of additional paralogues of some IRF family members in several teleost species [e.g. *Irf4a* and *Irf4b* in zebrafish (Stein *et al*., 2007)] is likely due to the whole genome duplication in the teleost lineage which occurred shortly after their divergence from lobe-finned fishes (Amores *et al*., 1998). Additional paralogues of IRF family genes may be present in salmonid species (e.g. IRF7A, IRF7B in Atlantic salmon, *Salmo salar*) as a result of the more recent genome duplication in that lineage (Lien *et al*., 2016 and references therein), although to our knowledge the entire IRF family has not yet been extensively studied in any salmonid species. Expansion of the vertebrate IRF gene family over evolutionary time is likely a factor in the observed diversity of function of these genes.

46 The amino (N) terminus of all vertebrate IRF proteins is well conserved, consisting of a
47 DNA-binding domain (DBD) approximately 115-120 amino acids in length, including five
48 conserved tryptophan (Trp) residues (Taniguchi *et al*., 2001). The DBD forms a helix-loop-helix
49 motif and recognizes the IFN stimulated response element (ISRE) in target genes, which has the
50 consensus sequence A/GNGAAANNGAAACT (Darnell *et al*., 1994) and is found in the
51 promoters of Type I IFNs and many ISGs. The carboxyl (C) terminus of IRF family members is
52 less conserved, except for an association module called the IRF associated domain (IAD) present
53 in all except *Irf1*and *Irf2,* which is important for interaction with other transcription factors
54 (Meraro *et al*., 1999).

55 In addition to their role in the IFN signalling pathway, IRF family members are known to
56 function in areas such as immune system regulation, growth, and development [see Ozato *et al*.,
57 2007; Savitsky *et al*., 2010; Matta *et al*., 2017 for reviews]. For example, while IRF1 is known as
58 a transcriptional activator of IFNα/β, mammalian studies have shown it is also required for DNA
59 damage-induced apoptosis, and is thus known as a tumor suppressor (Tanaka *et al*., 1996). IRF2
60 can be said to act opposite to IRF1, negatively regulating type I IFN responses (Honda and
61 Taniguchi 2006) and has been shown to have pro-oncogenic activity (reviewed by Yanai *et al*.,
62 2012). Comparatively little is known about IRF functions outside of innate immunity in fish
63 species, however, and further investigation could provide valuable insights into fish health and
64 development.

65 In contrast to all other IRF family members, IRF6 has not been shown to have a role in
66 IFN pathway regulation, though it is known to play a crucial role in the differentiation of
67 epithelia: mutations in human IRF6 lead to Van der Woude syndrome, or cleft palate (Kondo *et*
68 *al*., 2002), and in zebrafish and the frog *Xenopus laevis, Irf6* has been shown to be a maternal

69 transcript necessary for epithelial differentiation (Ben *et al*., 2005; Sabel *et al*., 2009). While
70 little is known about the roles of other IRF family members in early development of teleosts, *Irf7*
71 in *Gadus morhua* (*GmIrf7)* has been identified as a maternal transcript with a wide range of
72 expression in egg batches from different females (Rise *et al*., 2014). Transcript expression of
73 Atlantic cod *Irf1* (*GmIrf1*) and *GmIrf7* has also been observed to increase in early segmentation
74 stage cod embryos, suggesting that these genes may have stage-specific functions during early
75 development (Rise *et al*., 2012). Thus, in the current study we investigate the expression of all
76 IRF transcripts during early development, to identify any other maternal transcripts and predict
77 additional stage-specific roles.

78 In earlier reports we characterized *GmIrf1* (Feng *et al*., 2009), *GmIrf4a, GmIrf4b,*
79 Gm*Irf7*, *GmIrf8* and *GmIrf10* (Inkpen *et al*., 2015) in Atlantic cod, and showed that several of
80 these genes respond to immune stimulation (Rise *et al*., 2008; Hori *et al*., 2012). All previously
81 characterized IRFs in cod showed an expression response to stimulation with the virus-like
82 pathogen-associated molecular pattern (PAMP) polyriboinosinic polyribocytidylic acid
83 [poly(I:C)], a synthetic double stranded RNA. *GmIrf4b, GmIrf7, GmIrf8* and *GmIrf10* were also
84 responsive to stimulation with killed *Aeromonas salmonicida* (ASAL); furthermore, these
85 responses were seen to be modulated by elevated temperature (Hori *et al*., 2012; Inkpen *et al*.,
86 2015). Others have shown that several cod *Irf* transcripts also respond to nervous necrosis virus
87 infection in the brain, based on microarray analysis (Krasnov *et al*., 2013), and *GmIrf1* was
88 observed to respond to stimulation with heat-killed *Vibrio anguillarum* in the spleen (Caipang *et*
89 *al*., 2009).

90 IRF genes have been well characterized in several fish species in the past ~ decade [e.g.
91 in mandarin fish, *Siniperca chuasti* (Sun *et al*., 2007), rainbow trout, *Oncorhynchus mykiss*

92 (Holland *et al*., 2008), Atlantic salmon, (Bergan *et al*., 2010), rock bream, *Oplegnathus fasciatus*
93 (Bathige *et al*., 2012), orange spotted grouper, *Epinephelus coioides* (Huang *et al*., 2017), blunt
94 snout bream, *Megalobrama amblycephala* (Zhan *et al*., 2017), and zebrafish (Ben *et al*., 2005;
95 Xiang *et al*., 2010; Li *et al*., 2011)]; but most studies have investigated only one or two
96 transcripts at a time. However, the number of genome assemblies generated for non-model
97 organisms including teleost fish has been steadily increasing, which has facilitated more in-depth
98 characterizations of gene families of interest, contributing to our understanding of the evolution
99 of the unique immune system of Atlantic cod and its relatives (Star *et al*., 2011; Malmstrøm *et*
100 *al*., 2016). These studies show that the Gadiformes have lost important genes of the major
101 histocompatibility complex (MHC) II pathway, and harbour expansions of several important
102 immune gene families such as the MHC I and specific Toll-like receptors (TLRs) (Star *et al*.,
103 2011; Malmstrøm *et al*., 2016: Solbakken *et al.,* 2016; 2017). The characterization of all Atlantic
104 cod IRFs will allow us to determine if the composition of this gene family is similar to or
105 different from other species as they become more well studied within the teleost lineage.

106 In the current study, the remaining IRF family members (*GmIrf2, GmIrf3, GmIrf5,*
107 *GmIrf6, GmIrf9*) were predicted using the most recent Atlantic cod genome assembly [i.e.,
108 gadMor2, (Torresen *et al*., 2017)], and verified using the same methods as the previously
109 characterized Atlantic cod IRF transcripts [i.e., rapid amplification of cDNA ends (RACE), TA-
110 cloning, and sequencing (Feng *et al*., 2009; Inkpen *et al*., 2015)]. Constitutive expression of all
111 transcripts not previously studied was investigated in adult tissues using RT-PCR, and real-time
112 quantitative PCR (QPCR) was used to observe expression of all cod IRFs during embryonic
113 development, and to determine the expression response to viral and bacterial PAMP stimulation
114 in isolated macrophages.

2. Materials and Methods

2.1 cDNA characterization of cod IRF paralogues

Paralogue-specific RACE primers were designed for *GmIrf2, GmIrf3, GmIrf5, GmIrf6,* and *GmIrf9* (Table 1) based on predicted cDNA sequences from the Ensembl database (see web references), and on expressed sequence tag (EST) evidence as described previously (Inkpen *et al*., 2015).

Column-purified RNA was pooled from two adult cod spleen samples as well as poly(I:C)-stimulated macrophages isolated from head kidney (sampled at 24 h post-stimulation) and used for RACE. The experimental design, sampling procedures, and method of RNA preparation are described in sections 2.3 and 2.4. Five micrograms of pooled RNA were used to prepare RACE-ready cDNA using the GeneRacer Kit (Invitrogen, Burlington, ON, Canada), according to the manufacturer's instructions. RACE was carried out in 50 µL reactions containing 1 µL (1 U/µL) DyNAzyme polymerase (Thermo Scientific, Ottawa, ON, Canada), DyNAzyme EXT buffer (1X final concentration), and either reverse gene specific primer (GSP) and GeneRacer 5' primer or forward GSP and GeneRacer 3' primer for 5' RACE or 3' RACE, respectively. Touchdown PCR was carried out using an initial denaturation at 94°C for 2 min followed by 40 cycles of [30 s at 94°C; 30 s at 70°C→60°C, decreasing 0.3°C per cycle; 2 min at 72°C] and a final extension of 8 min at 72°C. Approximate size of PCR products was verified by agarose gel electrophoresis, and DNA bands were excised and purified using the QIAquick Gel Extraction Kit (QIAGEN, Mississauga, ON, Canada) as previously described (Inkpen *et al*., 2015).

RACE products were ligated into pGEM-T Easy vector (Promega, Madison, WI, USA) and replicated in Subcloning Efficiency DH5α chemically competent cells (Invitrogen) as previously described (Inkpen *et al*., 2015). Colonies containing recombinant plasmids with inserts were obtained by blue/white selection on LB agar/carbenicillin (50 μg/mL) plates containing 40 μL of 40 mg/mL X-gal (Sigma, Oakville, ON, Canada), and then grown overnight at 37°C with shaking at 225 rpm in liquid LB media containing 50 μg/mL carbenicillin. Plasmid DNA was isolated using the QIAprep Spin Miniprep Kit (QIAGEN), following the manufacturer's instructions. Each RACE product was sequenced in both directions using M13F and M13R primers with help of the staff at the GaP (Genomics and Proteomics) facility, CREAIT network, Memorial University of Newfoundland, as described previously (Inkpen *et al*., 2015). Sequencing reactions were processed by capillary electrophoresis using the Applied Biosystems 3730 DNA Analyzer.

2.2 Sequence analysis and comparison to genome assembly

Sequence data based on RACE was compiled and analyzed using Lasergene SeqMan Pro software V.7.1.0 (DNASTAR, Inc., Madison, WI, USA) and Sequencher V5.4.6 (Gene Codes Corporation, Ann Arbor, MI, USA). Amino acid sequences for each paralogue were predicted based on cDNA sequence using the ExPASy Translate tool (see Web References). Separately, the Atlantic cod genome assembly gadMor2 (Torresen *et al*., 2017) was scanned for all IRF-like sequences based on the previously characterized family members. For each gene, the putative transcript and genomic sequences were aligned using the BLAST 2 Sequences alignment tool (see Web References) to verify the transcript assembly and annotate intron/exon boundaries.

159 Following analysis, RACE PCR, cloning and sequencing of *GmIrf3*, *GmIrf5*, and *GmIrf9* were
160 repeated as the 5' and 3' untranslated regions (UTRs) of these transcripts appeared to be
161 incomplete.

162 Transcripts were further validated using the BLASTx alignment search tool with default
163 parameters (see Web References) to compare with IRF protein sequences of other teleost fish in
164 which this gene family has been fully or partially characterized. Homologous IRF protein
165 sequences from other teleost species [zebrafish, Atlantic salmon, rainbow trout, Japanese
166 flounder (*Paralichthys olivaceus*), grass carp (*Ctenopharyngodon idella*), rock bream] were
167 collected from the NCBI non-redundant (nr) protein database using the BLASTx alignment
168 search tool and Atlantic cod *Irf* transcripts as queries (see Supplemental Table 1). Predicted IRF
169 amino acid sequences were aligned with the ClustalW function of MEGA7 software (Kumar *et*
170 *al*., 2016). Based on the multiple sequence alignment, a phylogenetic tree was constructed using
171 the neighbour-joining method in MEGA7, where the bootstrap consensus tree was constructed
172 from 2000 replicates, and evolutionary distances were computed using the Poisson correction
173 method.
174

175 *2.3 RT-PCR expression analysis in Atlantic cod tissues*

176 All procedures involving sampling of early life stage or adult cod were conducted with
177 approval of Memorial University of Newfoundland's Institutional Animal Care Committee,
178 following the guidelines of the Canadian Council on Animal Care. In this experiment, two
179 juvenile Atlantic cod were individually removed from a flow-through tank (5.0-6.5ºC, 95-110%
180 oxygen saturation) and quickly euthanized by a lethal dose of tricaine methanesulfonate (TMS;
181 400 mg/L; Syndel Laboratories, Qualicum Beach, BC, Canada). Tissue samples (blood, brain,

182 eye, fin, gill, gonad, head kidney, heart, hindgut, liver, midgut, posterior kidney, pyloric caecum,
183 dorsal skeletal muscle, dorsal and ventral skin, spleen, stomach) were collected and immediately
184 flash-frozen in liquid nitrogen before storage at -80°C.
185 Total RNA was extracted from each tissue using TRIzol reagent (Invitrogen), and RNA
186 cleanup and cDNA synthesis were carried out as previously described (Inkpen *et al*., 2015).
187 Briefly, RNA was treated with DNaseI (QIAGEN) and column-purified using the RNeasy Mini
188 Kit (Invitrogen) following the manufacturer's instructions, and quality (A260/280 and
189 A260/230) and concentration were assessed by Nanodrop (Thermo Scientific)
190 spectrophotometry. One microgram of each clean RNA sample was used for cDNA synthesis
191 with M-MLV (Moloney Murine Leukemia Virus) reverse transcriptase (Invitrogen), following
192 the manufacturer's instructions.
193 Paralogue-specific primers for *GmIrf2-v1, GmIrf2-v2, GmIrf3, GmIrf5, GmIrf6* and
194 *GmIrf9* were designed using Primer3 software (see Web References) for use in all RT-PCR and
195 QPCR experiments (Table 2). RT-PCR was carried out using TopTaq DNA polymerase
196 (QIAGEN) as described in Inkpen *et al*. (2015). As in that study, *EF1α* (elongation factor 1 α)
197 was used as a reference gene, and for each primer set, a no-template control containing all
198 reaction components except cDNA was also run. PCR products were electrophoretically
199 separated on 1.7% agarose/TAE gels (stained with ethidium bromide) alongside 1 Kb Plus DNA
200 Ladder (Invitrogen).
201
202 *2.4 QPCR expression analysis in embryonic and larval development*
203 Adult (broodstock) Atlantic cod involved in this study were handled by the staff of the
204 Dr. Joe Brown Aquatic Research Building (JBARB) at the Ocean Sciences Centre of Memorial

University. After communal spawning, fertilized eggs were collected in 3 batches and ozonated at 1.5-2 ppm for 1.5 min and placed in three 250 L incubators with air stones. Temperature was recorded daily and maintained at 5-7 °C for the duration of sampling, and non-buoyant dead embryos and/or shells from hatched larvae were removed daily by draining from the bottom of each incubator before sampling. Each day from 0 to 17 days post-fertilization (dpf), 250 µL of embryos from each incubator were placed in a 1.5 mL RNase-free microcentrifuge tube, flash frozen in liquid nitrogen and stored at -80°C. Embryos were also observed under a light microscope to estimate developmental stage and confirm synchronous development, and pictures were taken of representative samples for each day (Supplemental Figure 1).

Total RNA was extracted, purified, and quality checked as above, and cDNA was prepared using M-MLV reverse transcriptase as above. Paralogue-specific primers (Table 2) for *GmIrf4a, GmIrf4b, GmIrf7, GmIrf8*, *GmIrf10-v1*, and *GmIrf10-v2* were developed and used in previous studies (Inkpen *et al*., 2015). All primer pairs were quality tested for the current study using pooled cDNA (i.e. 2 µg each of one sample from each time-point). For each assay, a 5-point, 4-fold dilution standard curve (starting with cDNA corresponding to 10 ng input RNA) was used to calculate amplification efficiency as described in Pfaffl (2001). Triplicate reactions were carried out for all standard curves, controls and experimental samples. The same pooled cDNA was also used as a linker in the QPCR study; this sample was included in all plates, and plates were only included for analysis if linker Ct values were within 1 cycle of each other.

All QPCR analyses were performed using SYBR Green chemistry and the 7500 Fast Real-Time PCR system (Applied Biosystems). Cycling conditions consisted of 1 cycle of 50˚C for 2 min, 1 cycle of 95˚C for 10 min, followed by 40 cycles of (95˚C for 15 s and 60˚C for 1 min), including a final melt curve stage for primer quality testing assays. QPCR assays were

carried out in 13 µL reactions containing 6.5 µL Power SYBR Green master mix (Applied Biosystems), 0.52 µL each of forward and reverse primers (50 nM final concentration), 3.46 µL nuclease-free water (Invitrogen) and 2.5 µL cDNA (corresponding to 12.5 ng input RNA). All samples were run as triplicate technical replicates, and no-template controls were included for each primer set in each plate. To confirm the absence of any genomic DNA, a "no reverse transcription" (no-RT) control was also included in which a mock cDNA synthesis reaction using the linker RNA pool was carried out with all components except reverse transcriptase. The no-RT reaction product was run in triplicate (2.5 µL of the no-RT reaction, as with cDNA samples), for each primer set, and no amplification was observed. Based on analysis of 4 potential normalizers with the geNorm algorithm of qbase+ software (Biogazelle Zwijnaarde, Belgium), *Tubb2* (tubulin beta 2A) and *EIF3* (eukaryotic initiation factor 3) were chosen as normalizers (geNorm M<0.5). Gene of interest (GOI) expression was normalized to the geometric mean of *Tubb2* and *EIF3* expression, and relative quantity (RQ) of each QPCR target transcript for each individual was calculated using the 7500 Fast Software (Applied Biosystems) for Comparative C_T ($\Delta\Delta C_T$) analysis (Livak and Schmittgen, 2001), incorporating calculated amplification efficiencies for each primer pair (Table 2). The sample with lowest normalized expression for each gene of interest was set as the calibrator (RQ set as 1.0) for analysis of that gene. RQ values were plotted using Prism v5.0 (GraphPad Software Inc., La Jolla, CA, USA).

2.5 QPCR expression analysis in immune-stimulated adherent head kidney macrophages

Atlantic cod macrophages were isolated as described by Eslamloo *et al*. (2016). Briefly, six adult Atlantic cod were euthanized as above, and the head kidney was removed by dissection and transferred to Leibovitz's 15+ [L-15 (Gibco, Carlsbad, CA) culture medium supplemented

with 2 mM L-glutamine, 4.2 mM $NaHCO_3$, 25 mM HEPES, 1.8 mM glucose, 20 U ml^{-1} heparin (Sigma-Aldrich, St. Louis, MO) and 100 U ml^{-1} penicillin and 100 µg ml^{-1} streptomycin (Gibco)]. The cells were passed through 100 µm nylon cell strainers (Fisherbrand™, Thermo Fisher Scientific, Waltham, MA), and the resulting cell suspension was centrifuged at 300 × g for 40 min at 4˚C on a 25%/51% Percoll gradient (GE Healthcare, Uppsala, Sweden) containing Hank's Balanced Salt Solution (HBSS; Thermo Fisher Scientific). The leukocytes were collected, and washed in L-15+, and placed in 35 mm culture dishes (Corning™, Corning, NY) at a density of 3 x 10^7 cells per dish (in 2 ml L-15+ containing 1% fetal bovine serum (FBS; Gibco) and no heparin). After ~24 h culture at 10˚C, the cells were washed 3 times to remove non-adherent cells, and samples of the adherent cells were observed microscopically to confirm the majority of cells showed macrophage morphology. Media was then replaced with 2 ml L-15+ containing 20 µg/mL poly(I:C) in phosphate buffered saline (PBS; Gibco), as in Eslamloo *et al*. (2016), 20 µg/mL LPS (*E. coli* O26:B6; Sigma-Aldrich; as in Seppola *et al*., 2015) in PBS, or 20 µl PBS. Sampling was carried out at 12, 24, 48, and 72 h post-stimulation (HPS), using aseptic techniques as described by Eslamloo *et al*. (2018), and samples were immediately stored at -80°C. Total RNA was extracted using *mirVana* miRNA isolation kit (Ambion, Life Technologies, Carlsbad, CA) according to the manufacturer's instruction. RNA quality was determined by agarose gel electrophoresis and Nanodrop spectrophotometry, and cDNA was prepared using M-MLV reverse transcriptase as previously described. QPCR reaction setup was performed as described above, except using 2 µL cDNA (corresponding to 10 ng input RNA). GOI expression was normalized to the geometric mean of *EF1α* and *rplp1* (acidic ribosomal protein P1) expression, (representing lowest geNorm M values (<0.4), following analysis of 4 potential normalizers), and RQs were calculated, analyzed and plotted as above.

3. Results

3.1 Characterization of GmIrf2-v1, GmIrf2-v2, GmIrf3, GmIrf5, GmIrf6 and GmIrf9 cDNA sequences

Two *GmIrf2* splice variants were identified in this study. Assembly of *GmIrf2-v1* sequencing reads produced a 1354 bp cDNA sequence (excluding poly-A tail) (Figure 1A, Supplemental Figure 2). The sequence consists of a 1062 bp (353 AA) open reading frame (ORF), a 258 bp 5' UTR, and a 33 bp 3'-UTR. Assembly of sequencing reads for the second *Irf2* variant (*GmIrf2-v2*) produced a 1572 bp cDNA sequence (excluding poly-A tail) (Figure 1B, Supplemental Figure 3), consisting of a 723 bp (240 AA) ORF, a 258 bp 5'-UTR, and a 591 bp 3'-UTR. The two transcripts are identical until exon 6, where *GmIrf2-v2* retains part of intron 6 and reaches a stop codon.

GmIrf3 sequencing reads were assembled to produce a 1323 bp transcript, consisting of a 1083 bp (360 AA) ORF, a 74 bp 5'-UTR, and 166 bp of the 3'-UTR (Figure 1C, Supplemental Figure 4). *GmIrf5* sequencing reads were assembled to produce a 1487 bp cDNA sequence that contains a 1233 bp (410 AA) ORF, a 140 bp 5'-UTR, and 114 bp of the 3'-UTR (Figure 1D; Supplemental Figure 5). Assembly of *GmIrf6* sequencing reads produced a 2475 bp cDNA sequence that consisted of a 1431 bp (476 AA) ORF, a 207 bp 5'-UTR and a 837 bp 3'-UTR (Figure 1E; Supplemental Figure 6). *GmIrf9* sequencing reads were assembled into a 1989 bp transcript, consisting of a 1284 bp ORF (427 AA), a 397 bp 5'-UTR, and a 308 bp 3'-UTR (Figure 1F; Supplemental Figure 7). It should be noted that the 3'UTR sequences of *Irf3* and *Irf5*

obtained using the methods described above (section 2.1) appeared to be incomplete, not reaching the expected poly-A tail.

Alignment of each transcript against its genomic sequence using the gadMor2 genome assembly (Torresen *et al*., 2017) allowed for the prediction of location and sizes of introns (Figure 1; Supplemental Figures 2-7). Phylogenetic analysis of Atlantic cod IRF proteins and those from selected other teleosts (Supplemental Table 1) indicated that all cod IRFs characterized in both the current and previous studies (Inkpen *et al*., 2015) were putatively orthologous to IRFs from other fish species. Multiple sequence alignment showed that the DBDs (first 110-120 AA) of all teleost IRF sequences included were quite similar, including well-conserved Trp residues found in all IRFs (Supplemental Figure 8). In a phylogenetic tree based on the multiple sequence alignment (Figure 2), all teleost IRF sequences grouped into the four sub-groups described above (IRF1-G, IRF3-G, IRF4-G, IRF5-G), as expected.

3.2 RT-PCR expression analysis in Atlantic cod tissues

GmIrf2, GmIrf3, GmIrf5, GmIrf6, and *GmIrf9* transcript expression was observed in 18 cod tissues using RT-PCR and agarose gel electrophoresis (Supplemental Figure 9). While most of these transcripts showed some expression in all tissues, *GmIrf6* appeared to be absent or show very low expression in blood, eye, brain, heart, spleen, and muscle (Supplemental Figure 9F). Notably, differences in expression were observed between the two *GmIrf2* splice variants identified in this study (Supplemental Figure 9B, C). The longer splice variant (*GmIrf2-v1*) showed more uniform expression in all tissues, while the shorter splice variant (*GmIrf2-v2*) appeared to have very low expression in the gonad, muscle and digestive system (i.e. stomach,

317 pyloric caecum, midgut, hindgut). *GmIrf5* also appeared to have lower expression in muscle and
318 tissues of the digestive system relative to other tissues (Supplemental Figure 9E).
319
320 *3.3 QPCR expression analysis in embryonic and early larval development*
321 Atlantic cod IRF transcripts showed distinct expression profiles during early development
322 (0-17 dpf). It should be noted that, while *Tubb2* and *EIF3* were chosen as acceptable normalizers
323 by geNorm analysis (section 2.4), expression of both transcripts in 0-1 dpf samples was lower
324 than at other time-points (normalizer Ct values are presented in Supplemental Table 2). The
325 overall expression profiles of *GmIrf1* and *GmIrf7* show some similarities (Figure 3A, I), both
326 peaking during segmentation (8-10 dpf for *GmIrf1* and 7-8 dpf for *GmIrf7*), though *GmIrf1*
327 expression was low overall and was in fact undetectable by QPCR in some stages. Splice
328 variants of *GmIrf2* again showed differences in constitutive expression (e.g. *GmIrf2-v1*
329 expression was highest at 2 dpf, while *GmIrf2-v2* expression was highest at 10 dpf; Figure 3B,
330 C), though it should be noted that variation in expression among biological replicates within
331 time-points was high. The two *GmIrf10* splice variants identified previously (Inkpen *et al*., 2015)
332 also had different expression profiles: *GmIrf10-v1* appeared to increase from 4-8 dpf, peaking
333 and then decreasing gradually, while *GmIrf10-v2* expression appeared to increase drastically at 2
334 dpf, remaining high through most of segmentation and dropping again at 11 dpf (Figure 3L, M).
335 Interestingly, the expression profile of *GmIrf4b* (Figure 3F) was very similar to that of *GmIrf10-*
336 *v2*, with relatively higher expression from 2-10 dpf, lower expression during hatching and an
337 apparent increase in expression post-hatch. *GmIrf5*, *GmIrf6*, and *GmIrf8* were all relatively
338 highly expressed in early cleavage stages (0-1 dpf), then dropped drastically and remained
339 relatively low for the rest of the study (Figure 3G, H, J). As noted above, the relatively low

expression of both normalizer transcripts at 0-1 dpf (Supplemental Table 2) may have impacted the presented RQ values at these time-points. Expression of *GmIrf3* showed a general decrease with time (Figure 3D), with lowest relative expression occurring during hatching (13-14 dpf), while *GmIrf4a* and *GmIrf9* transcripts both showed increases in expression over time, with highest relative expression in hatched larvae (15-17 dpf; Figure 3E, K).

3.4 QPCR expression analysis in immune-stimulated head kidney macrophages

The expression of all *Irf* transcripts in Atlantic cod macrophages stimulated with poly(I:C) or LPS was analyzed using QPCR at four time-points (12, 24, 48 and 72 HPS). To confirm that both treatments induced an immune response, additional antiviral (viperin, ISG15) and antibacterial (Il8, Il-1β) transcripts were also analyzed (Supplemental Figure 10), showing increased expression in response to poly(I:C) and LPS, respectively. Increased transcript expression of IFNγ in response to both treatments also indicates stimulation of interferon signalling pathways.

A summary of the observed *Irf* transcript responses in comparison with previous cod studies is presented in Table 3. Most transcripts were significantly up-regulated in response to poly(I:C) stimulation in at least one time-point, and none were down-regulated by poly(I:C) stimulation (Figure 4). Neither *GmIrf6* nor *GmIrf8* showed any significant difference in expression between the control (PBS-treated) and poly(I:C) treated cells, or within treatments at different time points. *GmIrf1* showed a higher expression in poly(I:C)-treated cells than PBS controls at 12 and 48 HPS; upregulation was also apparent at 24 h, but this difference was not statistically significant (Figure 4A). Once again, differences in expression were observed between *GmIrf2-v1* and *GmIrf2-v2* splice variants (Figure 4B, C). *GmIrf2-v1* transcript

363 expression was up-regulated in response to poly(I:C) treatment at all four time-points compared
364 with time-matched PBS controls, while *GmIrf2-v2* up-regulation was only observed at 24 HPS.
365 Expression of *GmIrf2-v2* was also observed to change in the control (PBS) cells, decreasing from
366 12 to 24 HPS. *GmIrf3* and *GmIrf7* transcript expression was up-regulated by poly(I:C) at all
367 time-points; the greatest increases (over 7-fold) in *GmIrf3* were observed at 48 and 72 HPS
368 (Figure 4D), while *GmIrf7* expression appeared to be most responsive to poly(I:C) at 12 and 24
369 HPS (8.4 and 10.3-fold, respectively; Figure 4I). Both *GmIrf4* paralogues showed similar up-
370 regulation in poly(I:C) stimulated cells compared to PBS controls at all time-points included in
371 the study (Figure 4E, F), while expression of *GmIrf4b* also differed significantly between 12 and
372 24 HPS PBS (control) samples. *GmIrf5* transcript expression was only slightly up-regulated (< 2-
373 fold) in response to poly(I:C) stimulation at 12 and 24 HPS, while no significant response was
374 observed at the later time-points (Figure 4G). Expression at 24 HPS was, however, significantly
375 lower than at any other time-point for *GmIrf5*, in both PBS and poly(I:C) treated cells. Very
376 similar expression profiles were observed for *GmIrf9* and *GmIrf10-v1* transcripts in response to
377 poly(I:C) stimulation (Figure 4K, L); as they were up-regulated at all time-points, with the
378 highest expression observed in poly(I:C) treated cells at 48 HPS (5.7-fold and 23.5-fold
379 upregulation in *GmIrf9* and *GmIrf10-v1,* respectively) and 72 HPS (4.7-fold and 20.9-fold
380 upregulation in *GmIrf9* and *GmIrf10-v1,* respectively). These transcripts also showed lower
381 expression in control samples at 24 HPS than at all other time-points. *GmIrf10-v1* showed the
382 greatest increase in expression overall, with over 20-fold upregulation in poly(I:C) treated cells
383 compared to PBS controls at 48 and 72 HPS. The shorter *GmIrf10* splice variant (*GmIrf10-v2*),
384 however, was only 1.7- and 2-fold up-regulated at 48 and 72 HPS respectively, and was non-
385 responsive to poly(I:C) at 12 and 24 HPS (Figure 4M).

386 Only 6 of 13 Atlantic cod *Irf* transcripts were LPS-responsive, each showing up-
387 regulation of 2-fold or less compared to time-matched PBS controls (Figure 5). *GmIrf1, GmIrf2-*
388 *v1, GmIrf3, GmIrf4a* and *GmIrf10-v2* were all up-regulated at only 72 HPS, while *GmIrf5* was
389 up-regulated only at 12 HPS. While *GmIrf2-v2* expression appeared to be up-regulated in
390 response to LPS at several time-points (Figure 5C), expression of this transcript varied widely
391 among individuals within treatment groups, and these changes were not statistically significant.
392 Both *GmIrf6* and *GmIrf8* were non-responsive to LPS (Figure 5H, J) as well as poly(I:C) as
393 noted above, and neither of these transcripts showed significant changes in expression among
394 time points. *GmIrf7* expression, while responsive to poly(I:C), showed no significant response to
395 LPS stimulation (Figure 5I). Notably, several transcripts (i.e. *GmIrf2-v1, GmIrf3, GmIrf4b,*
396 *GmIrf5, GmIrf9, GmIrf10-v1*) showed similar patterns of expression over time, wherein
397 expression decreased from 12 to 24 HPS and then increased from 24 HPS to 48 HPS in PBS
398 and/or LPS-treated cells (Figure 5B, D, F, G, K, L).

399

400 **4. Discussion**

401 *4.1 IRF transcript characterization and phylogenetic analysis*

402 Following the characterization of *GmIrf1, GmIrf4a, GmIrf4b, GmIrf7, GmIrf8* and
403 *GmIrf10* (Feng *et al*., 2009; Inkpen *et al*., 2015) by our research group, the objective of the
404 current study was to complete the characterization of all Atlantic cod IRF family member
405 transcripts. Six additional transcripts (*GmIrf2-v1, GmIrf2-v2, GmIrf3, GmIrf5, GmIrf6* and
406 *GmIrf9*) were identified and characterized at the cDNA and putative amino acid levels, and all
407 cod IRFs were compared with those of other teleost fish species by molecular phylogenetic

analysis. Long and short splice variants of Atlantic cod *Irf2* (*GmIrf2-v1* and *GmIrf2-v2,* respectively) were identified, and while analysis of the gadMor2 genome assembly also indicated an additional putative *Irf2* paralogue located on a scaffold region, this coding region was 99% identical to the RACE-identified *GmIrf2* located in linkage group (LG) 10 of the genome, suggesting a possible error in assembly rather than an additional gene copy. No other additional paralogues of the previously characterized cod IRFs were identified using the updated genome assembly.

Interestingly, similar to *GmIrf10-v2* (Inkpen *et al*., 2015), *GmIrf2-v2* appears to be produced by intron retention, leading to a truncated transcript. IRF family member splice variants, particularly in human research, have been shown to perform distinct roles mainly associated with disease. For example, multiple variants, including splice variants, of human *Irf5* have been associated with risk of developing systemic lupus erythematosus (Graham *et al*., 2007), and human *Irf1* splice variants were observed to negatively regulate wild type *Irf1* in cervical cancer tissue (Lee *et al.,* 2006). However, to our knowledge, differential splicing of either *Irf2* or *Irf10* has not been observed in any other fish species; therefore, it is difficult to predict the function of these shorter transcripts in cod. Furthermore, we have not yet investigated the expression of these variants at the protein level. Thus, further expression and functional studies are required to determine if *GmIrf2* and *GmIrf10* variants have different regulatory roles.

Multiple sequence alignment and phylogenetic analysis indicated that all Atlantic cod IRFs fall into the expected four sub-groups (IRF1-G, IRF3-G, IRF4-G, IRF5-G; as in Nehyba *et al*., 2002), and all contain the amino terminal DBD and associated conserved tryptophan residues common to all IRFs. As noted previously (Inkpen *et al*., 2015), teleost IRF7 orthologues appear to lack one Trp compared to all other orthologues, while teleost IRF1-G sequences (i.e. IRF1 and

IRF2) have an additional Trp residue in the DBD. As these conserved amino acids play an important role in binding the ISRE (Escalante *et al*., 1998), it is possible that variations may affect target gene specificity of IRF family members. When all Atlantic cod IRFs were compared, significant sequence variation was observed outside of the DBD, as expected (Supplemental Figure 8B). Variation in the IAD, at the carboxyl region of all IRF proteins except IRF1-G, is indicative of the wide range of functions of IRFs outside of IFN regulation, as this region is important for protein-protein interactions (Meraro *et al*., 1999). Thus, *GmIrf10-v2* for example, which lacks the IAD, is expected to function quite differently from *GmIrf10-v1*, as suggested by the expression profiles discussed below.

4.2 RT-PCR expression analysis in Atlantic cod tissues

All transcripts characterized in the current study appeared to be ubiquitously expressed in juvenile cod tissues except *GmIrf6,* which appeared to have little or no expression in some important immune related tissues such as the spleen and blood (Supplemental Figure 9F). This is consistent with our previous understanding of IRF6 function, as it has long been thought to be the only IRF family member without a known role in the innate immune response (Savitsky *et al*., 2010). IRF6 has been shown to be necessary for epithelial development in other species such as zebrafish and the frog *Xenopus laevis* (Ben *et al*., 2005; Sabel *et al*., 2009); expression of *GmIrf6* was observed in Atlantic cod tissues such as skin and gill (as well as fin, kidney, gonad, and gut), suggesting a role for IRF6 in those tissues in juvenile fish.

As with the previously identified *Irf10* splice variants (Inkpen *et al*., 2015), different expression patterns were observed among the *GmIrf2* variants based on RT-PCR analysis, with *GmIrf2-v1* appearing to be more ubiquitously expressed and more highly expressed overall

453 (Supplemental Figure 9B, C). IRF2 often acts as a transcriptional repressor, in opposition to
454 IRF1 and IRF9, and has been shown to be pro-oncogenic (Savitsky *et al*., 2010; Yanai *et al*.,
455 2012). Its potentially conserved role in the IFN pathway in cod, as with most other IRFs, is
456 supported by relatively high constitutive transcript expression in the spleen, head kidney, and
457 blood. The very low expression of *GmIrf2-v2* in the gonad and several areas of the gut suggests it
458 has a less significant role in those tissues than *GmIrf2-v1*; however, little is known of IRF2
459 function in these areas. Several cod IRF transcripts show ubiquitous expression in the tissues
460 studied (i.e. *GmIrf2-v1*, *GmIrf3, GmIrf9* in the current study and *GmIrf7, GmIrf8* and *GmIrf10-*
461 *v1* in Inkpen *et al*. 2015), suggesting more ubiquitous function of these transcription factors in
462 many cell types.

463 *4.3 QPCR expression analysis in embryonic and larval development*

464 All Atlantic cod IRF transcripts, characterized in our previous (Inkpen *et al*., 2015) and
465 current studies, were included in the QPCR study of early developmental expression herein.
466 Notably, most transcripts included in the current study showed high variation in expression
467 among biological replicate pools during early development. Our research group has previously
468 described high variation in *GmIrf7* transcript expression among egg batches from different
469 females in Atlantic cod (Rise *et al*., 2014), and thus while the replicates in the current study
470 represented pooled embryos from multiple parents (communally spawned), for future studies a
471 larger number of replicate batches from multiple parents may be useful. However, clear changes
472 in transcript expression over time were observed despite the limited sample size, suggesting
473 stage-specific functions of several transcripts.

GmIrf1 and *GmIrf7* were included in a previous study of embryonic transcript expression, using different egg batches from those used in the current study (Rise *et al*., 2012). The expression profiles observed for both transcripts, particularly *GmIrf7*, agreed well with the previous study, in both cases showing a peak in expression during segmentation (Figure 3A, I). Although there has been little study of IRF function during embryonic development in other species, a recent study of blunt snout bream (*Megalobrama amblycephala*) showed *Irf7* expression peaking during hatching (Zhan *et al*., 2017), and *Irf7* has been observed as a potential indicator of egg quality in both Atlantic halibut (*Hippoglossus hippoglossus* L) and sea bass (*Dicentrarchus labrax*), showing significantly higher expression in "high quality" egg or embryo groups than "low quality" groups (Mommens *et al*., 2014; Zarski *et al*., 2017). Contrary to those studies, previous analysis of Atlantic cod *Irf7* expression in fertilized and unfertilized eggs showed no correlation with egg quality (Rise *et al*., 2014). Thus, while our data suggest important roles for IRF7, IRF1, and potentially their target genes in the IFN pathway during early development, these roles may vary among teleost species. This study also supports previous research showing *GmIrf7* to be a maternal transcript (Rise *et al*., 2012; 2014), as expression was relatively high at 0-1 dpf. The lower expression observed at 2-5 dpf may indicate degradation of a maternal transcript during the maternal-to-zygotic transition (MZT; for review see Lee *et al*., 2014).

Several other Atlantic cod IRF transcripts show high relative expression at the earliest time-points studied (0-1 dpf) compared to later stage embryos, indicating potential maternal transcripts. As noted by Hall *et al*. (2004), Atlantic cod embryos at approximately 36 hours post fertilization (hpf) have entered the mid-blastula transition (MBT), during which the embryo begins to transcribe its own mRNA. Therefore, we may assume that transcripts with high

497 expression at 0-1 dpf are highly expressed in the unfertilized egg. Particularly, *GmIrf5*, *GmIrf6*,
498 and *GmIrf8* all showed dramatically higher expression at 0-1 dpf than at any time-point
499 thereafter (Figure 3G, H, J). Zebrafish IRF8 has been shown to function in embryonic
500 macrophage development (Shiau *et al*., 2015), though to our knowledge it has not been described
501 as a maternal transcript. Functional studies of *GmIrf8* (e.g. using morpholino knockdown in
502 Atlantic cod embryos or cultured macrophages) will be of interest in the future, to determine the
503 potential role of this transcript in early development and particularly in embryonic myelopoiesis.
504 *Irf6* has previously been described as a maternal transcript in zebrafish and *X. laevis,* and is
505 known to have important roles in embryonic development (Sabel *et al*., 2009). The authors of
506 that study showed that maternally-derived *Irf6* seems to be vital for epithelial differentiation,
507 whereas blocking expression of embryonic IRF6 had little effect. Similar knockdown studies of
508 *GmIrf6* should be performed in the future to determine if this role is conserved in Atlantic cod.

509

510 *4.4 QPCR expression analysis in immune-stimulated head kidney macrophages*

511 In previous reports, we have analyzed the transcript expression responses of *GmIrf1*,
512 *GmIrf4a, GmIrf4b, GmIrf7, GmIrf8, GmIrf10-v1* (identified as *Irf10* in most studies), and
513 *GmIrf10-v2* stimulated with poly(I:C) and/or killed *Aeromonas salmonicida* (ASAL) in immune
514 tissues (Rise *et al*., 2008; Feng *et al*., 2009; Hori *et al*., 2012; Inkpen *et al*., 2015; Eslamloo *et*
515 *al*., 2016). In the current study, all 13 identified Atlantic cod *Irf* transcripts were analyzed in
516 response to stimulation with either poly(I:C) or LPS (i.e. inducing an antiviral or antibacterial
517 cellular response, respectively) in isolated head kidney macrophages. It should be noted that the
518 minimal or absent response to LPS stimulation observed for many transcripts may indicate that

519 they have less importance to the antibacterial response than the antiviral response, but could also
520 be partially due to variation in the response to LPS compared to a live or killed bacterium. We
521 have observed, for example, different responses to LPS than to killed ASAL (see Table 3 for
522 comparison). As our group has discussed previously (Smith *et al*., 2018 and references therein),
523 most fish lack TLR4 as an LPS receptor, but do respond to immune stimulation with LPS
524 (Seppola *et al*., 2015 and references therein), perhaps through an as-yet uncharacterized
525 mechanism. Expression of Il-8 and Il-1β, commonly used as biomarkers of the antibacterial
526 response, were both increased in response to LPS (Supplemental Figure 10), indicating the LPS
527 stimulation in this study was effective. Protein contaminants in the LPS used may also have
528 contributed to the transcript expression response observed, as noted by Smith *et al*. (2018).

529 IRF1 has been well studied in vertebrates as a transcriptional activator of IFNα/β, whose
530 expression can be induced by IFNs and other cytokines, or by viral infection (reviewed in
531 Taniguchi *et al*. 2001), and we have previously indicated its role in the antiviral response of
532 Atlantic cod (see Table 3). In isolated macrophages, *GmIrf1* was significantly upregulated (> 5-
533 fold) in response to poly(I:C) at 12 and 48 HPS, though the response appeared to decrease or end
534 by 72 HPS (Figure 4A). The potential role of IRF1 in antibacterial responses is not well
535 understood, though we have observed up-regulation in response to ASAL stimulation in Atlantic
536 cod previously (Feng *et al*., 2009). In response to LPS, *GmIrf1* was up-regulated slightly (<2-
537 fold compared to PBS controls) and only at 72 HPS (Figure 5A).

538 Expression of both Atlantic cod *Irf2* splice variants increased in response to poly(I:C),
539 though while *GmIrf2-v1* was significantly up-regulated (2.5 to 4.5-fold) at all four time-points,
540 *GmIrf2-v2* up-regulation (2.3-fold) was only observed at 24 HPS (Figure 4B, C). *Irf2* has
541 previously been shown to be poly(I:C)-responsive in Atlantic salmon cell lines (Bergen *et al*.,

2010), in head kidney of orange-spotted grouper (Shi *et al*., 2010), in rainbow trout gonad cells (Collet *et al*., 2003), and in several grass carp tissues (Gu *et al*., 2015). However, it is notable that *Irf2* expression in salmon was not changed in response to infectious salmon anemia virus, unlike other *Irf* transcripts (Bergen *et al*., 2010). In LPS-stimulated Atlantic cod macrophages, *GmIrf2-v1* was significantly up-regulated (1.4-fold) only at 72 HPS, and while *GmIrf2-v2* expression appeared to be up-regulated at several time-points, these differences were not statistically significant (Figure 5B, C). *Irf2* was previously uncharacterized in Atlantic cod, and to our knowledge no studies have investigated *Irf2* splice variants *Irf2* in other fish species, while only one study has described IRF2 variants in mammalian cells (Koenig Merediz *et al*., 2000). Therefore, while the differences observed in response to poly(I:C) and LPS stimulation suggest different roles for the two variants in the cellular immune response, further functional studies will be required to elucidate these roles.

GmIrf3 was not fully characterized prior to this study, though we previously characterized the closely related *GmIrf7* and observed it to be slightly up-regulated in response to ASAL in the spleen (Inkpen *et al*., 2015), and more highly up-regulated in response to poly(I:C) in the spleen (Rise *et al*., 2008; Hori *et al*., 2012), and in head kidney macrophages (Eslamloo *et al*., 2016). In the current study, both *GmIrf3* and *GmIrf7* were significantly up-regulated in response to poly(I:C), though while *GmIrf3* was most responsive at later time-points (over 7-fold up-regulated at 48 and 72 HPS), *GmIrf7* showed the greatest increase (10.3 fold) at 24 HPS (Figure 4D, I). *Irf3* has previously been shown to be poly(I:C) responsive in Atlantic cod larvae cells (Krasnov *et al*., 2013), and in other teleost species [e.g. in rainbow trout (Holland et al., 2008), Atlantic salmon (Bergan *et al*., 2010), turbot, *Scophthalmus maximus* (Hu *et al*., 2011), and tilapia, *Oreochromis niloticus* (Gu *et al*., 2016)], though only the rainbow trout study

565 investigated macrophage expression. The roles of both IRF3 and IRF7 as important regulators of
566 the antiviral response are well understood in mammalian species; both IRF3 and IRF7 are
567 expressed in the cytosol, activated downstream of the TLR3-dependent pathway and then
568 translocate to the nucleus following activation in response to viral infection (Honda and
569 Taniguchi, 2006). Fish IRF3 and IRF7 appear to function similarly to mammalian orthologues in
570 the antiviral response. In all vertebrates, the mechanisms by which these genes may regulate
571 antibacterial responses are less understood. In the current study *GmIrf7* expression in cod
572 macrophages showed no response to LPS stimulation, while *GmIrf3* was slightly up-regulated
573 (1.4-fold) at only 72 HPS (Figure 5D, I).

574 The IRF5 sub-group (*Irf5, Irf6*) had, to our knowledge, never been studied in cod prior to
575 this study; and the function of IRF6 in most fish species is not well understood. The role of IRF5
576 in the teleost antiviral immune response, however, has been indicated in several species,
577 including Japanese flounder (Hu *et al*., 2012), tongue sole (*Cynoglossus semilaevis*; Zhang *et al*.,
578 2015), common carp (*Cyprinus carpio* L.; Zhu *et al*., 2016), and zebrafish (Ai *et al*., 2018). In
579 the current study, *GmIrf5* expression increased in response to poly(I:C) stimulation, though, only
580 less than 2-fold increases over time-matched PBS controls were observed (Figure 4G). *GmIrf5*
581 was also up-regulated in response to LPS, though only at the earliest time-point in the study (12
582 HPS; Figure 5G). Interestingly, this is similar to the expression profile observed for *Il-8*, a
583 commonly used biomarker for antibacterial responses (Supplemental Figure 10). Others have
584 shown *Irf5* expression to be responsive to bacterial infection in common carp (Zhu *et al*., 2016),
585 and tongue sole (Zhang *et al*., 2015), which along with the current study suggest that teleost
586 IRF5 may be important to the innate antibacterial response in addition to the antiviral immune
587 response.

588 *GmIrf6* expression showed no significant change in response to poly(I:C) and LPS
589 stimulation in Atlantic cod head kidney macrophages (Figure 4H; Figure 5H). While these
590 results are consistent with the current understanding that the primary function of IRF6 is in
591 epithelial development (Ben *et al*., 2005; Sabel *et al*., 2009), a few studies have shown evidence
592 of *Irf6* up-regulation in response to poly(I:C) in zebrafish (Li *et al*., 2016) and bacterial infection
593 in tongue sole (Zhang *et al*., 2015). Thus, further study of *GmIrf6* in additional tissues and in
594 response to additional viral and bacterial antigens and live pathogens is needed to rule out a role
595 in the cod innate immune response.

596 Within the IRF4 sub-group, we previously characterized two *Irf4* paralogues (*GmIrf4a*;
597 *GmIrf4b*), and *GmIrf8,* and saw that both *GmIrf4b* and *GmIrf8* expression increased slightly in
598 the spleen in response to poly(I:C) and ASAL, though *GmIrf8* expression initially decreased
599 slightly with ASAL stimulation (Inkpen *et al*., 2015). *GmIrf4a* in that study had no response to
600 ASAL, and a 2-fold decrease in response to poly(I:C). In the current study, *GmIrf8* had no
601 significant response to either poly(I:C) or LPS (Figure 4J; Figure 5J). When taken with the
602 previous study, this suggests that if this transcript does play a role in the cellular immune
603 response, it may be a more subtle role, and its functions as a constitutively expressed gene may
604 be more important. However, *Irf8* expression was responsive to poly(I:C) in several other teleost
605 species [rainbow trout (Holland *et al*., 2010), rock bream (Bathidge *et al*., 2012), turbot (Chen *et*
606 *al*., 2012, and Japanese flounder (Hu *et al*., 2013)], suggesting our observations of *GmIrf8*
607 expression may be unique to Atlantic cod, though notably those studies did not investigate
608 expression in isolated macrophages. Both *GmIrf4a* and *GmIrf4b* increased in expression with
609 poly(I:C) stimulation at all time-points in the current study (Figure 4E, F), differing from our
610 observations in the spleen as noted above. Interestingly, the response of these paralogues to LPS

611 was somewhat opposite to the response observed to ASAL in the spleen (Inkpen *et al*., 2015), as
612 *GmIrf4b* had no response, and *GmIrf4a* showed only a 1.6-fold increase at 72 HPS (Figure 5E,
613 F). Further studies may help determine if these differences are indicative of tissue- or cell-
614 specific functions. IRF4 and IRF8 have been shown in mammalian species to have important
615 roles in myelopoiesis and the differentiation of macrophages (Tamura *et al*., 2015 and references
616 therein; Nam and Lim, 2016 and references therein), and similar function of IRF8 has also been
617 observed in zebrafish (Li *et al*., 2011). Although we have not yet determined if this function is
618 conserved in Atlantic cod, it would support the hypothesis that *GmIrf8* is less involved in the
619 macrophage antiviral and antibacterial responses and more important to other processes.

620 Atlantic cod *Irf10* was also shown to be immune responsive in our previous experiments
621 (Hori *et al*., 2012; Inkpen *et al*., 2015), with increased expression in response to both poly(I:C)
622 and ASAL in the spleen. Xu *et al.* (2016) also showed IRF10 in three different teleost species
623 [rainbow trout (two paralogues), grass carp, and swamp eel, *Monopterus albus*] to be responsive
624 to viral infection and/or poly(I:C). In the current study, both *GmIrf10* splice variants were up-
625 regulated in response to poly(I:C) stimulation, though while *GmIrf10-v1* expression was
626 increased at all time-points and showed the highest fold changes in the study (up to 23.5-fold;
627 Figure 4L), *GmIrf10-v2* was only up-regulated at 48 HPS and 72 HPS, and only showed a ~2-
628 fold increase (Figure 4M). With LPS stimulation, *GmIrf10-v1* showed no significant response,
629 while *GmIrf10-v2* increased in expression slightly (< 2-fold) at 72 HPS (Figure 5L, M).
630 Similarly, *GmIrf10-v2* was slightly more responsive than *GmIrf10-v1* to ASAL in the spleen
631 (Inkpen *et al*., 2015), though both variants showed some increase in expression in that study.
632 Collectively, these studies may suggest that the two variants have different roles in the innate

633 immune response, with *GmIrf10-v1* potentially acting more in the antiviral response and
634 *GmIrf10-v2* in the antibacterial response.

635 IRF9 has not previously been studied in Atlantic cod, though its role in the IFN pathway
636 has been well studied in mammalian species – it forms the ISGF3 transcription factor complex
637 along with STAT1 and STAT2, which activates several IFN pathway genes (Taniguchi *et al*.,
638 2001; Yanai *et al*., 2012, and references therein). To our knowledge IRF9 has only been studied
639 in a few teleost species, but within those studies it has been shown to be up-regulated in response
640 to IFN stimulation in zebrafish (Shi *et al*., 2013), in response to poly(I:C) and/or viral infection
641 in Japanese flounder (Hu *et al*., 2014), tongue sole (Zhang *et al*., 2015), miiuy croaker, *Miichthys*
642 *miiuy* (Yang *et al*., 2017), and mandarin fish (Laghari *et al*., 2018), and in response to bacterial
643 infection in tongue sole (Zhang *et al*., 2015) and blunt snout bream (Zhan *et al*., 2017). In the
644 current study, *GmIrf9* showed increased expression in response to poly(I:C) at all time-points,
645 but had no significant response to LPS (Figure 4K; Figure 5K). As noted above, further study of
646 the fish response to LPS, along with the use of live bacterial infection and other bacterial
647 antigens, would be valuable to better understand any potential roles of *Irf9* and other IRFs in the
648 teleost antibacterial response.

649

650 **Conclusions:**

651 In total, we have now characterized 13 IRF transcripts in Atlantic cod, completing the
652 characterization of this gene family at the transcript and hypothetical amino acid levels. All cod
653 IRF transcripts appear to be constitutively expressed in multiple tissues, and all were observed to
654 be expressed during embryonic and early larval development. These findings suggest potential
655 roles for IRF family members in Atlantic cod outside of their function in the innate antiviral

response, which may be similar to those observed in other vertebrate species. Immune stimulation of isolated Atlantic cod macrophages with poly(I:C) produced increases in expression of all but two IRF transcripts, including several transcripts which had been previously uncharacterized and therefore not shown to be immune responsive prior to this study. Several IRF transcripts were also responsive to stimulation with bacterial LPS, suggesting roles in the innate antibacterial response.

Acknowledgments:

This study was supported by a Natural Sciences and Engineering Research Council of Canada (NSERC) Discovery Grant to MLR. The genomic analyses were supported by The Research Council of Norway (Grant number 222378/F20) and performed on the Abel Supercomputing Cluster (Norwegian metacenter for High Performance Computing (NOTUR) and the University of Oslo) operated by the Research Computing Services group at USIT, the University of Oslo IT-Department (http://www.hpc.uio.no/). The authors would like to thank the Dr. Joe Brown Aquatic Research Building (JBARB) staff (Ocean Sciences Centre, Memorial University, NL), for their assistance with fish husbandry, Atefeh Ghorbani for help with tissue sampling, and Heather Fifield for assistance with sequencing.

675 **References:**

676 Ai K, Luo K, Xia L, Gao W, Hu W, Qi Z, Xu Q. 2018. Functional characterization of interferon
677 regulatory factor 5 and its role in the innate antiviral immune response. Fish Shellfish Immunol
678 72:31-36.

679 Amores A, Force A, Yan Y, Joly L, Amemiya C, Fritz A, Ho RK, Langeland J, Prince V, Wang
680 Y, Westerfield M, Ekker M, Postlethwait JH. 1998. Zebrafish *hox* clusters and vertebrate
681 genome evolution. Science 282:1711-14.

682 Bathige SDNK, Whang I, Umasuthan N, Lim BS, Park MA, Kim E, Park HC, Lee J. 2012.
683 Interferon regulatory factors 4 and 8 in rock bream, *Oplegnathus fasciatus*: Structural and
684 expressional evidence for their antimicrobial role in teleosts. Fish Shellfish Immunol 33:857-71.

685 Ben J, Wang Jabs E, and Chong SS. 2005. Genomic, cDNA and embryonic expression analysis
686 of zebrafish IRF6, the gene mutated in the human oral clefting disorders Van der Woude and
687 popliteal pterygium syndromes. Gene Expression Patterns 5:629-38.

688 Bergan V, Kileng Ø, Sun B, Robertsen B. 2010. Regulation and function of interferon regulatory
689 factors of Atlantic salmon. Mol Immunol 47:2005-14.

690 Caipang CM, Brinchmann MF, Kiron V. 2009. Profiling gene expression in the spleen of
691 Atlantic cod, *Gadus morhua* upon vaccination with *Vibrio anguillarum* antigen. Comp Biochem
692 Physiol B Biochem Mol Biol 153(3):261-67.

693 Chen X, Hu G, Dong X, Liu Q, Zhang S. 2012. Molecular cloning and expression analysis of
694 interferon regulatory factor 8 (IRF8) in turbot, *Scophthalmus maximus*. Vet Immunol
695 Immunopathol 149(1-2):143-50.

696 Collet B, Hovens GCJ, Mazzoni D, Hirono I, Aoki T, Secombes CJ. 2003. Cloning and
697 expression analysis of rainbow trout *Oncorhynchus mykiss* interferon regulatory factor 1 and 2
698 (IRF-1 and IRF-2). Dev Comp Immunol 27(2):111-26.

699 Darnell JE, Kerr IM, Stark GR. 1994. Jak-STAT pathways and transcriptional activation in
700 response to IFNs and other extracellular signaling proteins. Science 264:1415-21.

701 Escalante CR, Yie J, Thanos D, Aggarwal AK. 1998. Structure of IRF-1 with bound DNA
702 reveals determinants of interferon regulation. Nature 319:103-06.

703 Eslamloo K, Xue X, Booman M, Smith NC, Rise ML. 2016. Transcriptome profiling of the
704 antiviral immune response in Atlantic cod macrophages. Dev Comp Immunol 63:187-205.

705 Eslamloo K, Inkpen SM, Rise ML, Andreassen R. 2018. Discovery of microRNAs associated
706 with the antiviral immune response of Atlantic cod macrophages. Mol Immunol 93:152-61.

Feng CY, Johnson SC, Hori TS, Rise M, Hall JR, Gamperl AK, Hubert S, Kimball J, Bowman S, Rise ML. 2009. Identification and analysis of differentially expressed genes in immune tissues of Atlantic cod stimulated with formalin-killed, atypical *Aeromonas salmonicida*. Physiol Genomics 37(3):149-63.

Graham RR, Kyogoku C, Sigurdsson S, Vlasova IA, Davies LRL, Baechler EC, Plenge RM, Koeuth T, Ortmann WA, Hom G, et al., 2007. Three functional variants of IFN regulatory factor 5 (IRF5) define risk and protective haplotypes for human lupus. Proc Natl Acad Sci USA 104:6758-63.

Gu M, Lin G, Lai Q, Zhong B, Liu Y, Mi Y, Chen H, Wang B, Fan L, Hu C. 2015. *Ctenopharyngodon idella* IRF2 plays an antagonistic role to IRF1 in transcriptional regulation of IFN and ISG genes. Dev Comp Immunol 49(1):103-12.

Gu YF, Wei Q, Tang SJ, Chen XW, Zhao JL. 2016. Molecular characterization and functional analysis of IRF3 in tilapia (*Oreochromis niloticus*). Dev Comp Immunol 55:130-7.

Hall TE, Smith P, Johnson IA. 2004. Stages of embryonic development in the Atlantic cod *Gadus morhua*. J Morphol 259(3):255-0.

Holland JW, Bird S, Williamson B, Woudstra C, Mustafa A, Wang T, Zou J, Blaney SC, Collet B, Secombes CJ. 2008. Molecular characterization of IRF3 and IRF7 in rainbow trout, *Oncorhynchus mykiss*: Functional analysis and transcriptional modulation. Mol Immunol 46:269-85.

Holland JW, Karim A, Wang T, Alnabulsi A, Scott J, Collet B, Mughal MS, Secombes CJ, Bird S. 2010. Molecular cloning and characterization of interferon regulatory factors 4 and 8 (IRF-4 and IRF-8) in rainbow trout, *Oncorhynchus mykiss*. Fish Shellfish Immunol 29(1):157-66.

Honda K and Taniguchi T. 2006. IRFs: Master regulators of signalling by Toll-like receptors and cytosolic pattern-recognition receptors. Nat Rev Immunol 6:644-58.

Hori TS, Gamperl AK, Booman M, Nash GW, Rise ML. 2012. A moderate increase in ambient temperature modulates the Atlantic cod (*Gadus morhua*) spleen transcriptome response to intraperitoneal viral mimic injection. BMC Genomics 13:431.

Hu GB, Xia J, Lou HM, Chen XL, Li J, Liu QM. 2011. An IRF-3 homolog that is up-regulated by DNA virus and poly I:C in turbot, *Scophthalmus maximus*. Fish Shellfish Immunol 31(6):1224-31.

Hu GB, Lou HM, Dong XZ, Liu QM, Zhang SC. 2012. Characteristics of the interferon regulatory factor 5 (IRF5) and its expression in response to LCDV and poly I:C challenges in Japanese flounder, *Paralichthys olivaceus*. Dev Comp Immunol 38(2):377-82.

740 Hu G, Chen X, Gong Q, Liu Q, Zhang S, Dong X. 2013. Structural and expression studies of
741 interferon regulatory factor 8 in Japanese flounder, *Paralichthys olivaceus*. Fish Shellfish
742 Immunol 35(3):1016-24.

743 Hu GB, Zhao MY, Lin JY, Liu QM, Zhang SC. 2014. Molecular cloning and characterization of
744 interferon regulatory factor 9 (IRF9) in Japanese flounder, *Paralichthys olivaceus*. Fish Shellfish
745 Immunol 39(2):138-44.

746 Huang B, Qi Z, Xu Z, Nie P. 2010. Global characterization of interferon regulatory factor (IRF)
747 genes in vertebrates: Glimpse of the diversification in evolution. BMC Immunol 11:22.

748 Huang WS, Zhu MH, Chen S, Wang ZW, Liang Y, Huang B, Nei P. 2017. Molecular cloning
749 and expression analysis of a fish specific interferon regulatory factor, IRF11, in orange spotted
750 grouper, *Epinephelus coioides*. Fish Shellfish Immunol 60:368-379.

751 Inkpen SM, Hori TS, Gamperl AK, Nash GW, Rise ML. 2015. Characterization and expression
752 analyses of five interferon regulatory factor transcripts (Irf4a, Irf4b, Irf7, Irf8, Irf10) in Atlantic
753 cod (*Gadus morhua*). Fish Shellfish Immunol 44(1):365-81.

754 Koenig Merediz SA, Schmidt M, Hoppe GJ, Alfken J, Meraro D, Levi BZ, Neubauer A, Wittig
755 B. 2000. Cloning of an interferon regulatory factor 2 isoform with different regulatory ability.
756 Nucleic Acids Res 28(21):4219-24.

757 Kondo S, Schutte BC, Richardson RJ, Bjork BC, Knight AS, Watanabe Y, Howard E, Ferreira
758 de Lima RL, Daack-Hirsch S, *et al*. 2002. Mutations in IRF6 cause Van der Woude and popliteal
759 pterygium syndromes. Nature Genetics 32:285-89.

760 Krasnov A, Kileng O, Skugor S, Jorgensen SM, Afanasyev S, Timmerhaus G, Sommer AI,
761 Jensen I. 2013. Genomic analysis of the host response to nervous necrosis virus in Atlantic cod
762 (*Gadus morhua*) brain. Mol Immunol 54:443-52.

763 Kumar S, Stecher G, Tamura K (2016). MEGA7: Molecular Evolutionary Genetics Analysis
764 version 7.0 for bigger datasets. Mol Biol Evol 33:1870-1874.

765 Laghari ZA, Li L, Chen SN, Huo HJ, Huang B, Zhou Y, Nie P. 2018. Composition and
766 transcription of all interferon regulatory factors (IRFs), IRF1−11 in a perciform fish, the
767 mandarin fish, *Siniperca chuatsi*. Dev Comp Immunol 81:127-40.

768 Lee E, Jo M, Park J, Zhang W, Lee J. 2006. Alternative splicing variants of IRF-1 lacking exons
769 7, 8, and 9 in cervical cancer. Biochem Biophys Res Comm 347:882-88.

770 Lee MT, Bonneau AR, Giraldez AJ. 2014. Zygotic genome activation during the maternal-to-
771 zygotic transition. Annu Rev Cell Dev Biol 30:581-613.

772 Li L, Jin H, Xu J, Shi Y, Wen Z. 2011. Irf8 regulates macrophage versus neutrophil fate during
773 zebrafish primitive myelopoiesis. Blood 117:1359-69.

774 Li S, Lu LF, Wang ZX, Chen DD, Zhang YA. 2016. Fish IRF6 is a positive regulator of IFN
775 expression and involved in both of the MyD88 and TBK1 pathways. Fish Shellfish Immunol
776 57:262-68.

777 Lien S, Koop BF, Sandve SR, Miller JR, Kent MP, Nome T, et al. 2016. The Atlantic salmon
778 genome provides insights into rediploidization. Nature 533(7602):200-5.

779 Livak KJ, Schmittgen TD. 2001. Analysis of relative gene expression data using real-time
780 quantitative PCR and the 2(-Delta Delta C(T)) method. Methods 25:402–8.

781 Malmstrøm M, Matschiner M, Tørresen OK, Star B, Snipen LG, Hansen TF, Baalsrud HT,
782 Nederbragt AJ, Hanel R, Salzburger W, Stenseth NC, Jakobsen KS, Jentoft S. 2016. Evolution of
783 the immune system influences speciation rates in teleost fishes. Nat Genet 48:1204-10.

784 Matta B, Song S, Li D, Barnes BJ. 2017. Interferon regulatory factor signaling in autoimmune
785 disease. Cytokine 98:15-26.

786 Meraro D, Hashmueli S, Koren B, Azriel A, Oumard A, Kirchhoff S, Hauser H, Nagulapalli S,
787 Atchison ML, Levi B. 1999. Protein-protein and DNA-protein interactions affect the activity of
788 lymphoid-specific IFN regulatory factors. J Immunol 163:6468-78.

789 Mommens M, Fernandes JMO, Tollefsen KE, Johnston IA, Babiak I. 2014. Profiling of the
790 embryonic Atlantic halibut (*Hippoglossus hippoglossus* L.) transcriptome reveals maternal
791 transcripts as potential markers of embryo quality. BMC Genomics 15:829.

792 Nam S, Lim JS. 2016. Essential role of interferon regulatory factor 4 (IRF4) in immune cell
793 development. Arch Pharm Res 39(11):1548-55.

794 Nehyba J, Hrdlickova R, Burnside J, Bose HR. 2002. A novel interferon regulatory factor (IRF),
795 IRF-10, has a unique role in immune defense and is induced by the v-Rel oncoprotein. Mol Cell
796 Biol 22:3942-57.

797 Nehyba J, Hrdlickova R, Bose HR. 2009. Dynamic evolution of immune system regulators: The
798 history of the interferon regulatory factor family. Mol Biol Evol 26:2539-50.

799 Ozato K, Tailor P, Kubota T. 2007. The interferon regulatory factor family in host defense:
800 mechanism of action. J Biol Chem 282:20065-69.

801 Pfaffl M.W. 2001. A new mathematical model for relative quantification in real-time RT-PCR.
802 Nucleic Acids Res 29(9):e45.

803 Rise ML, Hall J, Rise M, Hori T, Gamperl AK, Kimball J, Hubert S, Bowman S, Johnson SC.
804 2008. Functional genomic analysis of the response of Atlantic cod (*Gadus morhua*) spleen to the
805 viral mimic polyriboinosinic polyribocytidylic acid (pIC). Dev Comp Immunol 32:916-31.

806 Rise ML, Hall JR, Alcock BP, Hori TS. 2012. Dynamic expression profiles of virus-responsive
807 and putative antimicrobial peptide-encoding transcripts during Atlantic cod (*Gadus morhua*)
808 embryonic and early larval development. Gene 509:232-46.

809 Rise ML, Nash GW, Hall JR, Booman M, Hori TS, Trippel EA, Gamperl AK. 2014. Variation in
810 embryonic mortality and maternal transcript expression among Atlantic cod (*Gadus morhua*)
811 broodstock: a functional genomics study. Marine Genomics Pt A 3-20.

812 Sabel JL, d'Alençon C, O'Brien EK, Otterloo EV, Lutz K, Cuykendall TN, Schutte BC, Houston
813 DW, Cornell RA. 2009. Maternal interferon regulatory factor 6 is required for the differentiation
814 of primary superficial epithelia in Danio and Xenopus embryos. Dev Biol 325:249-62.

815 Savitsky D, Yanai H, Taniguchi T. 2010. Regulation of immunity and oncogenesis by the IRF
816 transcription factor family. Cancer Immunol Immunother 59:489-510.

817 Seppola M, Mikkelsen H, Johansen A, Steiro K, Myrnes B, Nilsen IW. 2015. Ultrapure LPS
818 induces inflammatory and antibacterial responses attenuated in vitro by exogenous sera in
819 Atlantic cod and Atlantic salmon. Fish Shellfish Immunol 44(1):66-78.

820 Shi Y, Zhao Z, Yin JK, Zhu XP, Chen KC, Pan DB, Gui JF. 2010. Interferon regulatory factor-2
821 in orange-spotted grouper (*Epinephelus coioides*): Gene, inductive expression pattern and
822 subcellular localization. Comp Biochem Physiol B Biochem Mol Biol 155(2):110-17.

823 Shi J, Zhang YB, Zhang JS, Gui JF. 2013. Expression regulation of zebrafish interferon
824 regulatory factor 9 by promoter analysis. Dev Comp Immunol 41(4):534-43.

825 Shiau CE, Kaufman Z, Meireles AM, Talbot WS. 2015. Differential requirement for irf8 in
826 formation of embryonic and adult macrophages in zebrafish. PLoS One 10(1):e0117513.

827 Smith NC, Christian SL, Taylor RG, Santander J, Rise ML. 2018. Immune modulatory
828 properties of 6-gingerol and resveratrol in Atlantic salmon macrophages. Mol Immunol 95:10-
829 19. Corrigendum: Smith NC *et al.* 2018. Mol Immunol 104:139.

830 Solbakken MH, Rise ML, Jakobsen KS, Jentoft S. 2016. Successive losses of central immune
831 genes characterize the Gadiformes' alternate immunity. Genome Biol Evol 8(11):3508-15.

832 Solbakken MH, Voje KL, Jakobsen KS, Jentoft S. 2017. Linking species habitat and past
833 palaeoclimatic events to evolution of the teleost innate immune system. Proc Biol Sci
834 284(1853):20162810.

835 Star B, Nederbragt AJ, Jentoft S, Grimholt U, Malmstrøm M, Gregers TF, *et al*. 2011. The
836 genome sequence of Atlantic cod reveals a unique immune system. Nature 477(7363):207-10.

837 Stein C, Caccamo M, Laird G, Leptin M. 2007. Conservation and divergence of gene families
838 encoding components of innate immune response systems in zebrafish. Genome Biol 8:R251.

839 Sun BJ, Chang MX, Song Y, Yao WJ, Nie P. 2007. Gene structure and transcription of IRF-1
840 and IRF-7 in the mandarin fish *Siniperca chuatsi*. Vet Immunol Immunopathol 116:26-36.

841 Tamura T, Kurotaki D, Koizumi S. 2015. Regulation of myelopoiesis by the transcription factor
842 IRF8. Int J Hematol 101(4):342-51.

843 Tanaka N, Ishihara M, Lamphier MS, Nozawa H, Matsuyama T, Mak TW, Aizawa S, Tokino T,
844 Oren M, Taniguchi T. 1996. Cooperation of the tumor suppressors IRF-1 and p53 in response to
845 DNA damage. Nature 382(6594):816-18.

846 Taniguchi T, Ogasawara K, Takaoka A, Tanaka N. 2001. IRF family of transcription factors as
847 regulators of host defense. Annu Rev Immunol 19:623-55.

848 Torresen OK, Star B, Jentoft S, Reinar WB, Grove H, Miller JR, Walenz BP, Knight J, Ekholm
849 JM, Peluso P, Edvardsen RB, Tooming-Klunderud A, Skage M, Lien S, Jakobsen KS,
850 Nederbragt AJ. 2017. An improved genome assembly uncovers prolific tandem repeats in
851 Atlantic cod. BMC Genomics 18:95.

852 Xiang Z, Dong C, Qi L, Chen W, Huang L, Li Z, Xia Q, Liu D, Huang M, Weng S, *et al.,* 2010.
853 Characteristics of the interferon regulatory factor pairs zfIRF5/7 and their stimulation expression
854 by ISKNV infection in zebrafish (*Danio rerio*). Dev Comp Immunol 34:1263-73.

855 Xu Q, Jiang Y, Wangkahart E, Zou J, Chang M, Yang D, Secombes CJ, Nie P, Wang T. 2016.
856 Sequence and Expression Analysis of Interferon Regulatory Factor 10 (IRF10) in Three Diverse
857 Teleost Fish Reveals Its Role in Antiviral Defense. PLoS One 11(1):e0147181.

858 Yanai H, Negishi H, Taniguchi T. 2012. The IRF family of transcription factors: inception,
859 impact and implications in oncogenesis. OncoImmunology 1(8):1376-86.

860 Yang Q, Cui J, Song W, Zhao X, Xu T. 2017. The evolution and functional characterization of
861 miiuy croaker interferon regulatory factor 9 involved in immune response. Fish Shellfish
862 Immunol 66:524-30.

863 Żarski D, Nguyen T, Le Cam A, Montfort J, Dutto G, Vidal MO, Fauvel C, Bobe J. 2017.
864 Transcriptomic Profiling of Egg Quality in Sea Bass (*Dicentrarchus labrax*) Sheds Light on
865 Genes Involved in Ubiquitination and Translation. Mar Biotechnol 19:102-15.

866 Zhan FB, Liu H, Lai RF, Jakovlic I, Wang WM. 2017. Expression and functional
867 characterization of interferon regulatory factors (*irf2, irf7* and *irf9*) in the blunt snout bream
868 (*Megalobrama amblycephala*). Dev Comp Immunol 67:239-248.

869 Zhang J, Li YX, Hu YH. 2015. Molecular characterization and expression analysis of eleven
870 interferon regulatory factors in half-smooth tongue sole, *Cynoglossus semilaevis.* Fish Shellfish
871 Immunol 44(1):272-82.

872 Zhu Y, Qi C, Shan S, Zhang F, Li H, An L, Yang G. 2016. Characterization of common carp
873 (*Cyprinus carpio L.*) interferon regulatory factor 5 (IRF5) and its expression in response to viral
874 and bacterial challenges. BMC Vet Res 12(1):127.

875

876 **Web References**

877 *http://bioinfo.ut.ee/primer3-0.4.0/*; Web interface for Primer3.

878 *https://blast.ncbi.nlm.nih.gov/Blast.cgi*; National Center for Biotechnology Information BLAST
879 web interface (BLASTx; BLASTn; BLAST 2 sequences).

880
881 *http://web.expasy.org/translate/*; Web interface for ExPASy Translate tool.

882 *http://www.ensembl.org/*; Ensembl genome browser web interface.

884

885 **Figure Legends:**

886 **Figure 1: Schematic structure of Atlantic cod *Irf2-v1, Irf2-v2, Irf3, Irf5, Irf6,* and *Irf9*.**
887 Exons (E) are depicted as shaded boxes, where 1 cm represents 100 bp. 5' and 3' untranslated
888 regions (UTR) and introns (I) are depicted as lines. Introns longer than 150 bp and UTRs are
889 represented by bent lines (not to scale). A portion of I6 in *Irf2-v1* is expressed in E6 of *Irf2-v2*,
890 and is shaded black. Intron lengths are inferred from the gadMor2 genome assembly.

891

892 **Figure 2: Phylogenetic analysis of teleost IRF sequences.** Putative Atlantic cod amino acid
893 sequences were aligned with IRF proteins from other teleost fish species (see Supplemental
894 Table 1 for GenBank accession numbers) using MEGA7 software (Kumar *et al*., 2016). Based
895 on the multiple sequence alignment, the evolutionary history was inferred using the neighbour-
896 joining method. The bootstrap consensus tree was constructed from 2000 replicates, where
897 numbers at the branch points represent percentage of replicates in which the associated taxa
898 grouped together. Branch lengths are proportional to calculated evolutionary distances. Atlantic
899 cod sequences determined by our group in the current and previous studies are indicated by an
900 asterisk.

901

902 **Figure 3: Atlantic cod transcript expression of IRF family members throughout embryonic**
903 **and early larval development, measured by QPCR.** Data is presented as mean +/- SEM, of 3
904 pools normalized to the geometric mean of *Tubb2* and *EIF3* expression, with the lowest
905 expressing sample set to RQ=1. Normalizer Ct values are presented in Supplemental Table 2.

906 Developmental stages at each sampling point (x-axis) are based on observations and photographs
907 taken daily using light microscopy (Supplemental Figure 1), with reference to the work of Hall *et*
908 *al*. (2004).

909 **Figure 4: Atlantic cod macrophage transcript expression response of IRF family members**
910 **to poly(I:C), measured by QPCR.** Data is presented as mean +/- SEM, normalized to the
911 geometric mean of *EF1α* and *rplp1* expression, with the lowest expressing sample set to RQ=1.
912 Normalizer Ct values are presented in Supplemental Table 2. Note that *Irf1* expression is
913 represented as $\log_2$ of RQ, due to the wide range of RQ values observed for that transcript. An
914 asterisk (*) represents a significant difference between a poly(I:C) stimulated group and the
915 time-matched PBS group ($p < 0.05$). [** = $p<0.01$; *** = $p<0.001$; **** = $p<0.0001$]. Capital
916 letters and lower case letters represent similarity among PBS-treated groups and poly(I:C)-
917 treated groups across time points, respectively. Fold change is calculated as [mean poly(I:C)
918 RQ/mean PBS RQ].

919

920 **Figure 5: Atlantic cod macrophage transcript expression response of IRF family members**
921 **to LPS, measured by QPCR.** Data is presented as mean +/- SEM, normalized to the geometric
922 mean of *EF1α* and *rplp1* expression, with the lowest expressing sample set to RQ=1. Normalizer
923 Ct values are presented in Supplemental Table 2. Note that *Irf1* expression is represented as $\log_2$
924 of RQ, due to the wide range of RQ values observed for that transcript. An asterisk (*) represents
925 a significant difference between a poly(I:C) stimulated group and the time-matched PBS group
926 ($p < 0.05$). Capital letters and lower case letters represent similarity among PBS-treated groups

927 and LPS-treated groups across time points, respectively. Fold change is calculated as (mean LPS
928 RQ)/(mean PBS RQ).

929

930

A) IRF2-v1

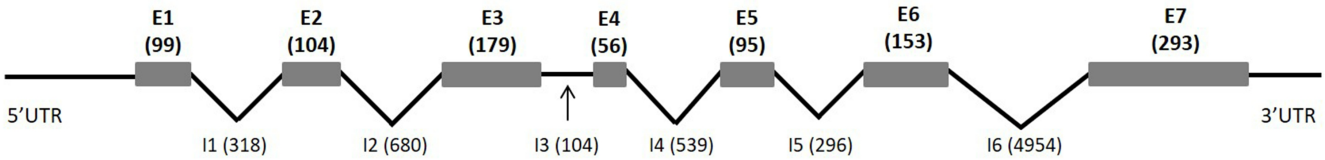

B) IRF2-v2

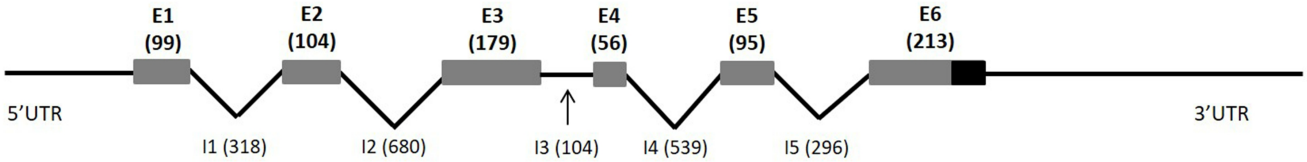

C) IRF3

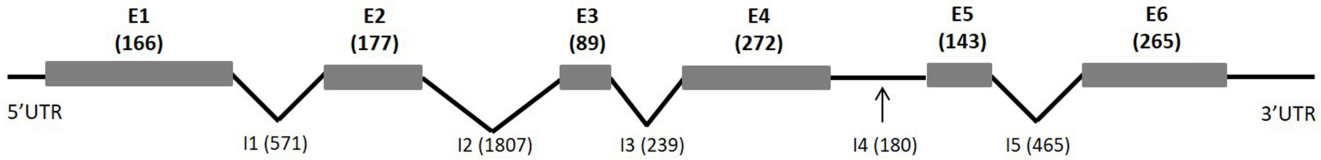

D) IRF5

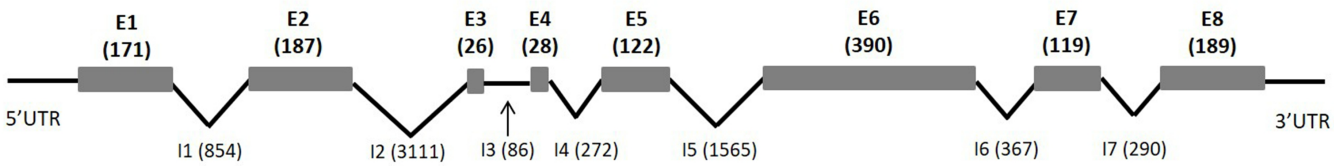

E) IRF6

F) IRF9

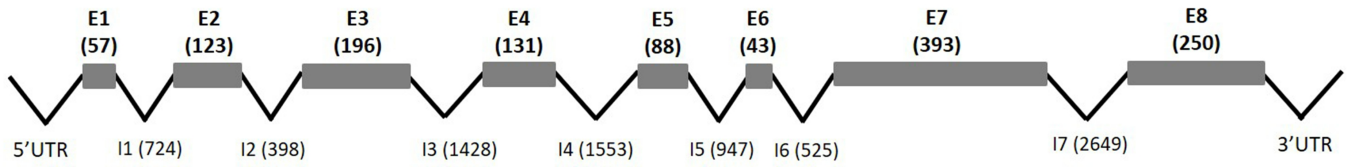

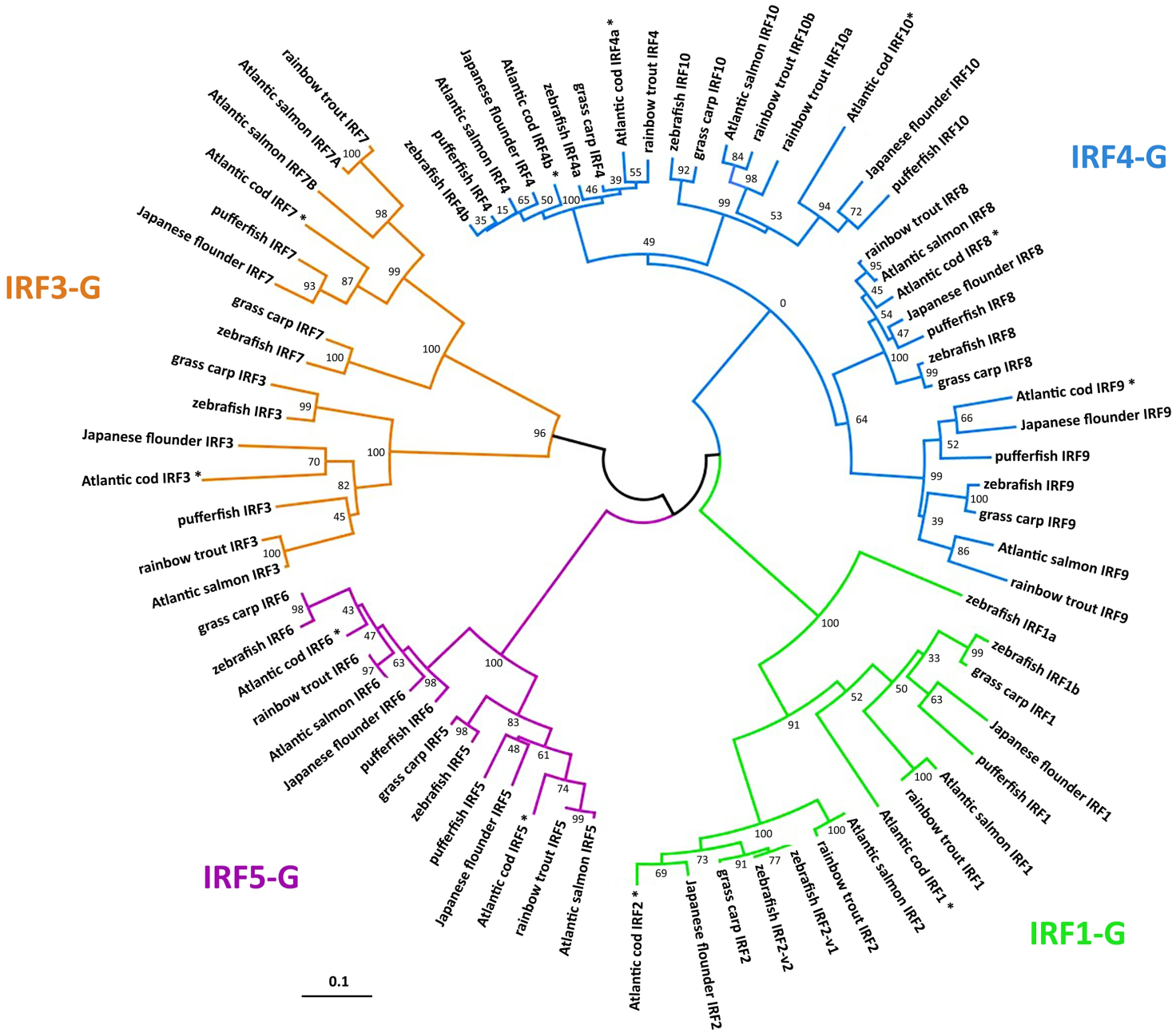
IRF3-G
IRF4-G
IRF5-G
IRF1-G
rainbow trout IRF7
Atlantic salmon IRF7A
Atlantic salmon IRF7B
Atlantic cod IRF7 *
pufferfish IRF7
Japanese flounder IRF7
grass carp IRF7
zebrafish IRF7
grass carp IRF3
zebrafish IRF3
Japanese flounder IRF3
Atlantic cod IRF3 *
pufferfish IRF3
rainbow trout IRF3
Atlantic salmon IRF3
grass carp IRF6
zebrafish IRF6
Atlantic cod IRF6 *
rainbow trout IRF6
Atlantic salmon IRF6
Japanese flounder IRF6
pufferfish IRF6
grass carp IRF5
zebrafish IRF5
pufferfish IRF5
Japanese flounder IRF5
Atlantic cod IRF5 *
rainbow trout IRF5
Atlantic salmon IRF5
Atlantic cod IRF2 *
Japanese flounder IRF2
grass carp IRF2
zebrafish IRF2-v2
zebrafish IRF2-v1
rainbow trout IRF2
Atlantic salmon IRF2
Atlantic cod IRF1 *
rainbow trout IRF1
Atlantic salmon IRF1
pufferfish IRF1
Japanese flounder IRF1
grass carp IRF1
zebrafish IRF1b
zebrafish IRF1a
rainbow trout IRF9
Atlantic salmon IRF9
grass carp IRF9
zebrafish IRF9
pufferfish IRF9
Japanese flounder IRF9
Atlantic cod IRF9 *
grass carp IRF8
zebrafish IRF8
pufferfish IRF8
Japanese flounder IRF8
Atlantic cod IRF8 *
Atlantic salmon IRF8
rainbow trout IRF8
pufferfish IRF10
Japanese flounder IRF10
Atlantic cod IRF10*
rainbow trout IRF10a
rainbow trout IRF10b
Atlantic salmon IRF10
grass carp IRF10
zebrafish IRF10
rainbow trout IRF4
Atlantic cod IRF4a *
grass carp IRF4
zebrafish IRF4a
Atlantic cod IRF4b *
Japanese flounder IRF4
Atlantic salmon IRF4
pufferfish IRF4
zebrafish IRF4b
0.1

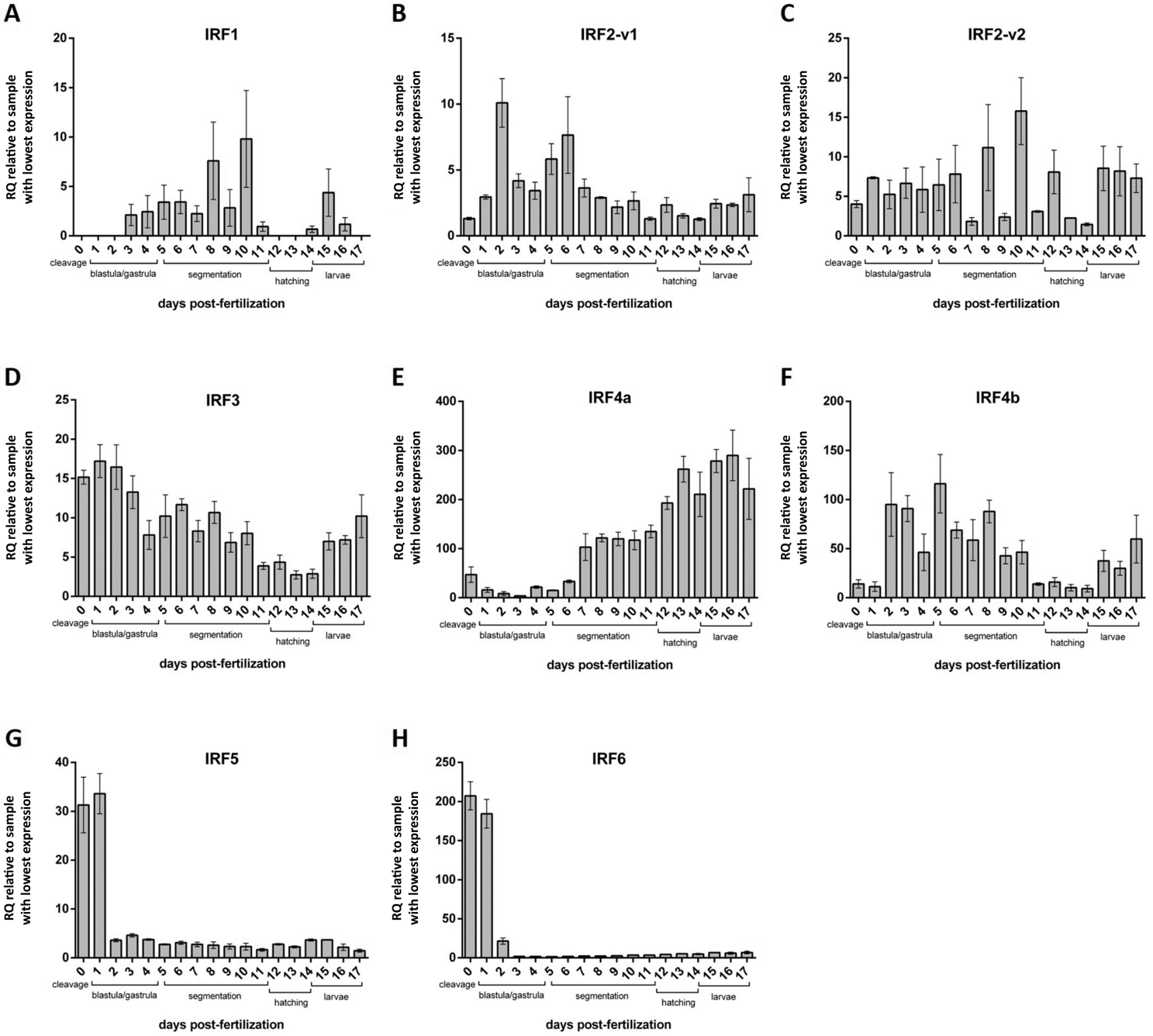
A
IRF1
B
IRF2-v1
C
IRF2-v2
D
IRF3
E
IRF4a
F
IRF4b
G
IRF5
H
IRF6
RQ relative to sample with lowest expression
cleavage
blastula/gastrula
segmentation
hatching
larvae
days post-fertilization

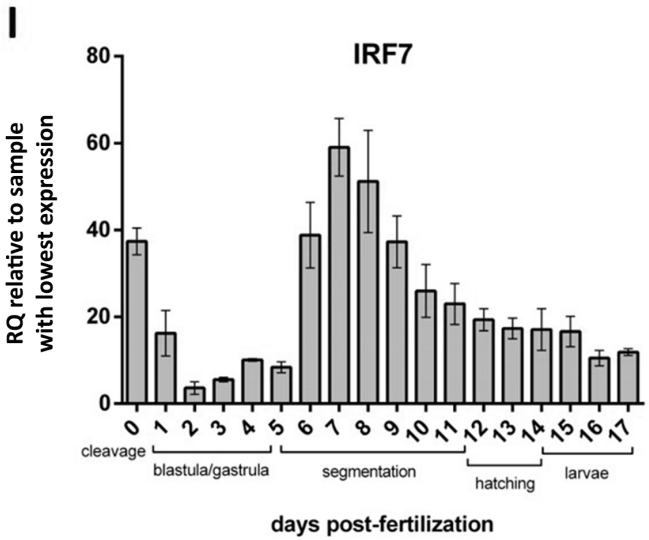
I
IRF7
RQ relative to sample with lowest expression
80
60
40
20
0
0 1 2 3 4 5 6 7 8 9 10 11 12 13 14 15 16 17
cleavage
blastula/gastrula
segmentation
hatching
larvae
days post-fertilization

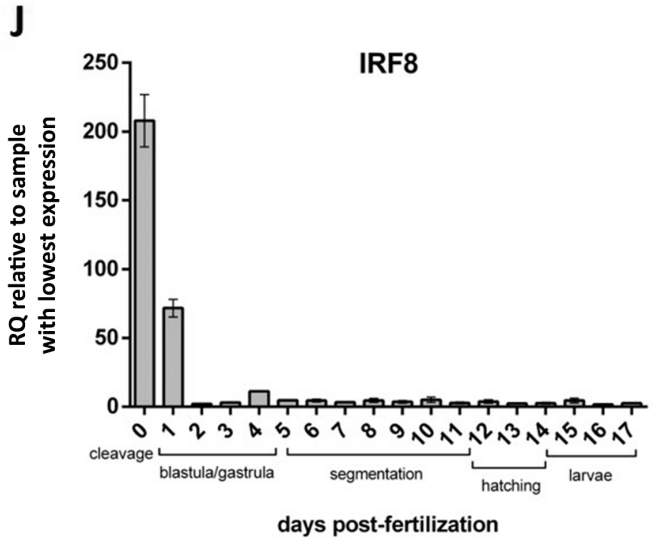
J
IRF8
RQ relative to sample with lowest expression
250
200
150
100
50
0
0 1 2 3 4 5 6 7 8 9 10 11 12 13 14 15 16 17
cleavage
blastula/gastrula
segmentation
hatching
larvae
days post-fertilization

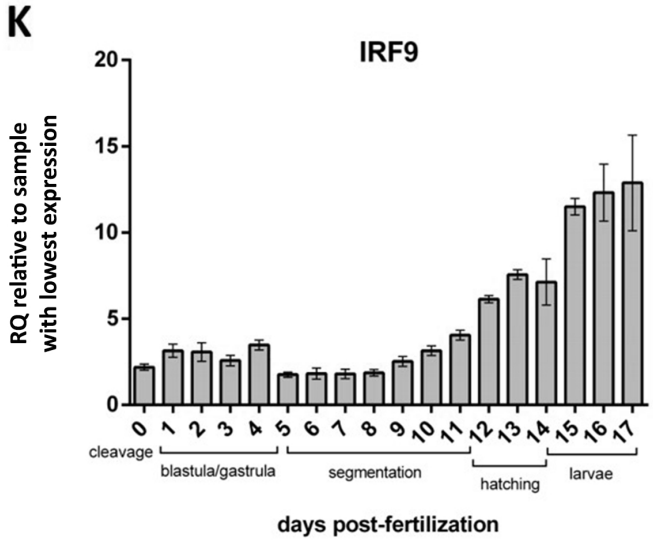
K
IRF9
RQ relative to sample with lowest expression
20
15
10
5
0
0 1 2 3 4 5 6 7 8 9 10 11 12 13 14 15 16 17
cleavage
blastula/gastrula
segmentation
hatching
larvae
days post-fertilization

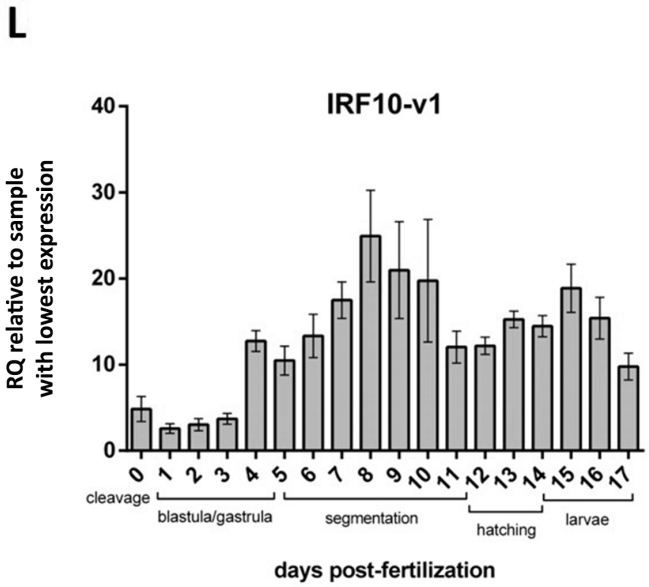
L
IRF10-v1
RQ relative to sample with lowest expression
40
30
20
10
0
0 1 2 3 4 5 6 7 8 9 10 11 12 13 14 15 16 17
cleavage
blastula/gastrula
segmentation
hatching
larvae
days post-fertilization

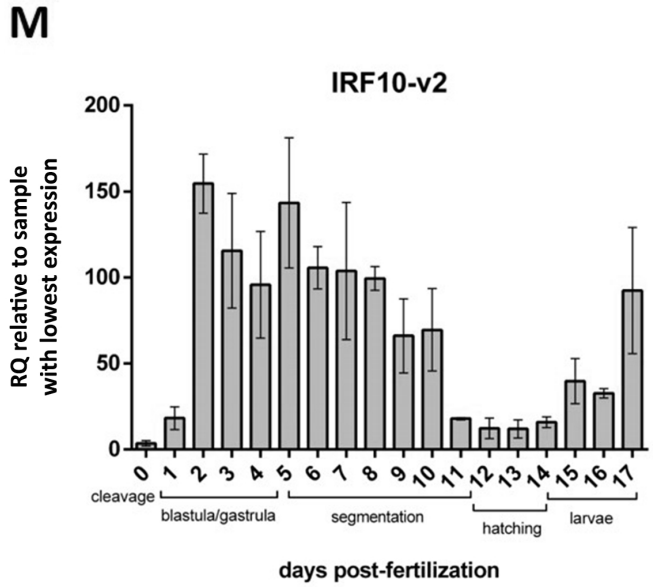
M
IRF10-v2
RQ relative to sample with lowest expression
200
150
100
50
0
0 1 2 3 4 5 6 7 8 9 10 11 12 13 14 15 16 17
cleavage
blastula/gastrula
segmentation
hatching
larvae
days post-fertilization

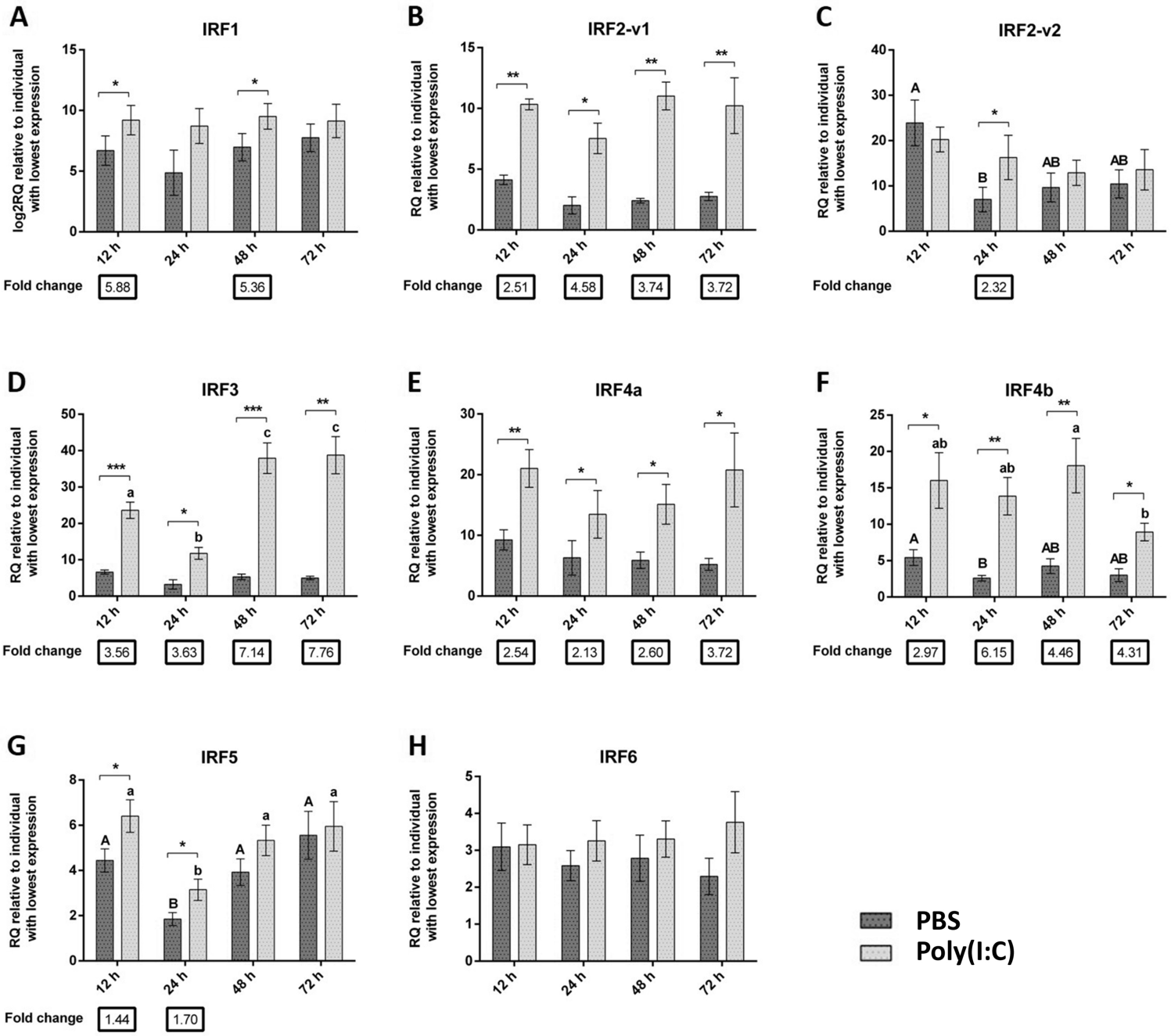
A
IRF1
log2RQ relative to individual with lowest expression
Fold change
5.88
5.36
B
IRF2-v1
RQ relative to individual with lowest expression
Fold change
2.51
4.58
3.74
3.72
C
IRF2-v2
RQ relative to individual with lowest expression
Fold change
2.32
D
IRF3
RQ relative to individual with lowest expression
Fold change
3.56
3.63
7.14
7.76
E
IRF4a
RQ relative to individual with lowest expression
Fold change
2.54
2.13
2.60
3.72
F
IRF4b
RQ relative to individual with lowest expression
Fold change
2.97
6.15
4.46
4.31
G
IRF5
RQ relative to individual with lowest expression
Fold change
1.44
1.70
H
IRF6
RQ relative to individual with lowest expression
12 h
24 h
48 h
72 h
PBS
Poly(I:C)

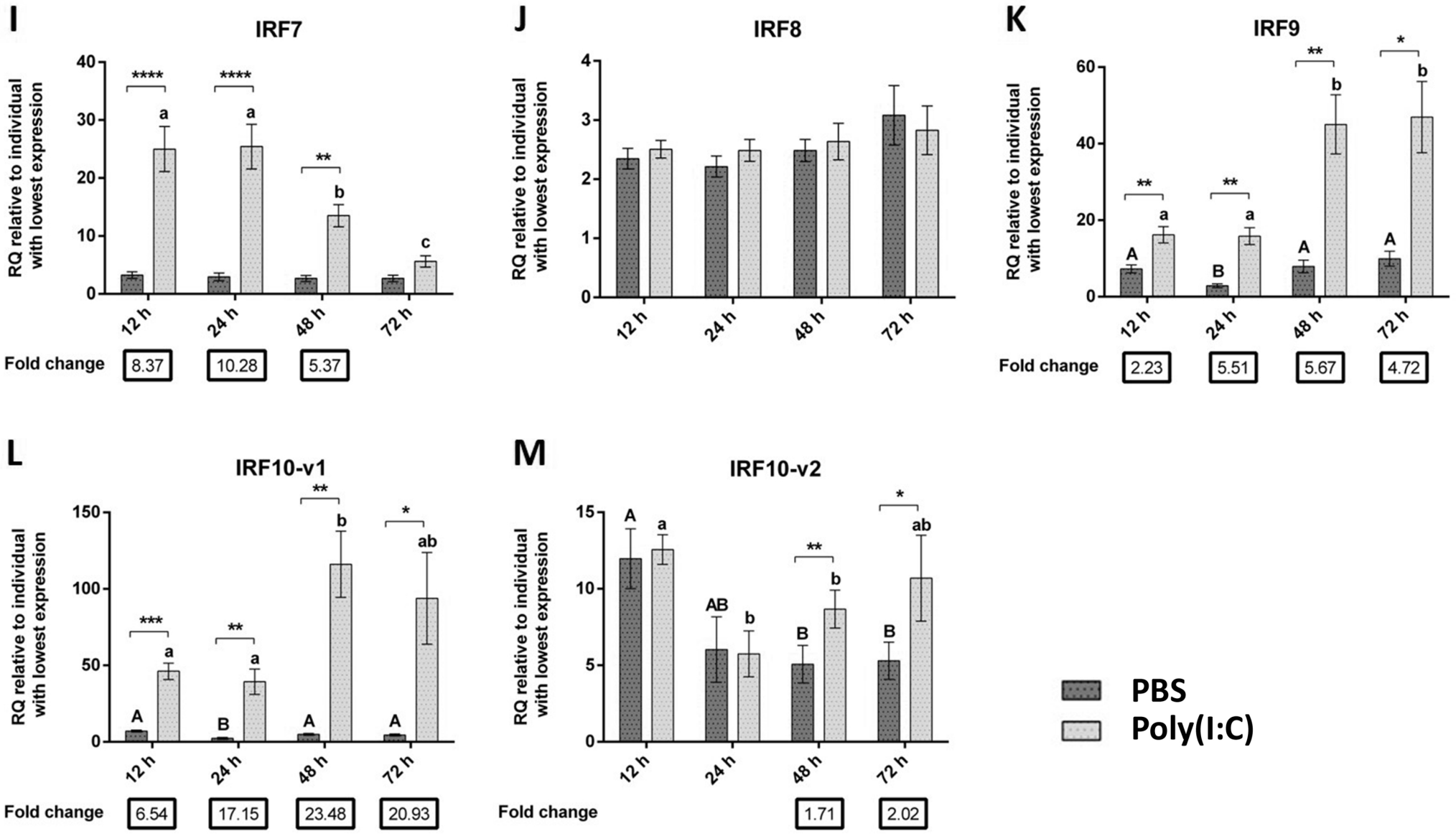
I
IRF7
RQ relative to individual with lowest expression
40
30
20
10
0
****
****
**
a
a
b
c
12 h
24 h
48 h
72 h
Fold change
8.37
10.28
5.37
J
IRF8
RQ relative to individual with lowest expression
4
3
2
1
0
12 h
24 h
48 h
72 h
K
IRF9
RQ relative to individual with lowest expression
60
40
20
0
**
**
**
*
A
a
B
a
A
b
A
b
12 h
24 h
48 h
72 h
Fold change
2.23
5.51
5.67
4.72
L
IRF10-v1
RQ relative to individual with lowest expression
150
100
50
0
***
**
**
*
A
a
B
a
A
b
A
ab
12 h
24 h
48 h
72 h
Fold change
6.54
17.15
23.48
20.93
M
IRF10-v2
RQ relative to individual with lowest expression
15
10
5
0
A
a
AB
b
B
b
B
ab
*
**
12 h
24 h
48 h
72 h
Fold change
1.71
2.02
PBS
Poly(I:C)

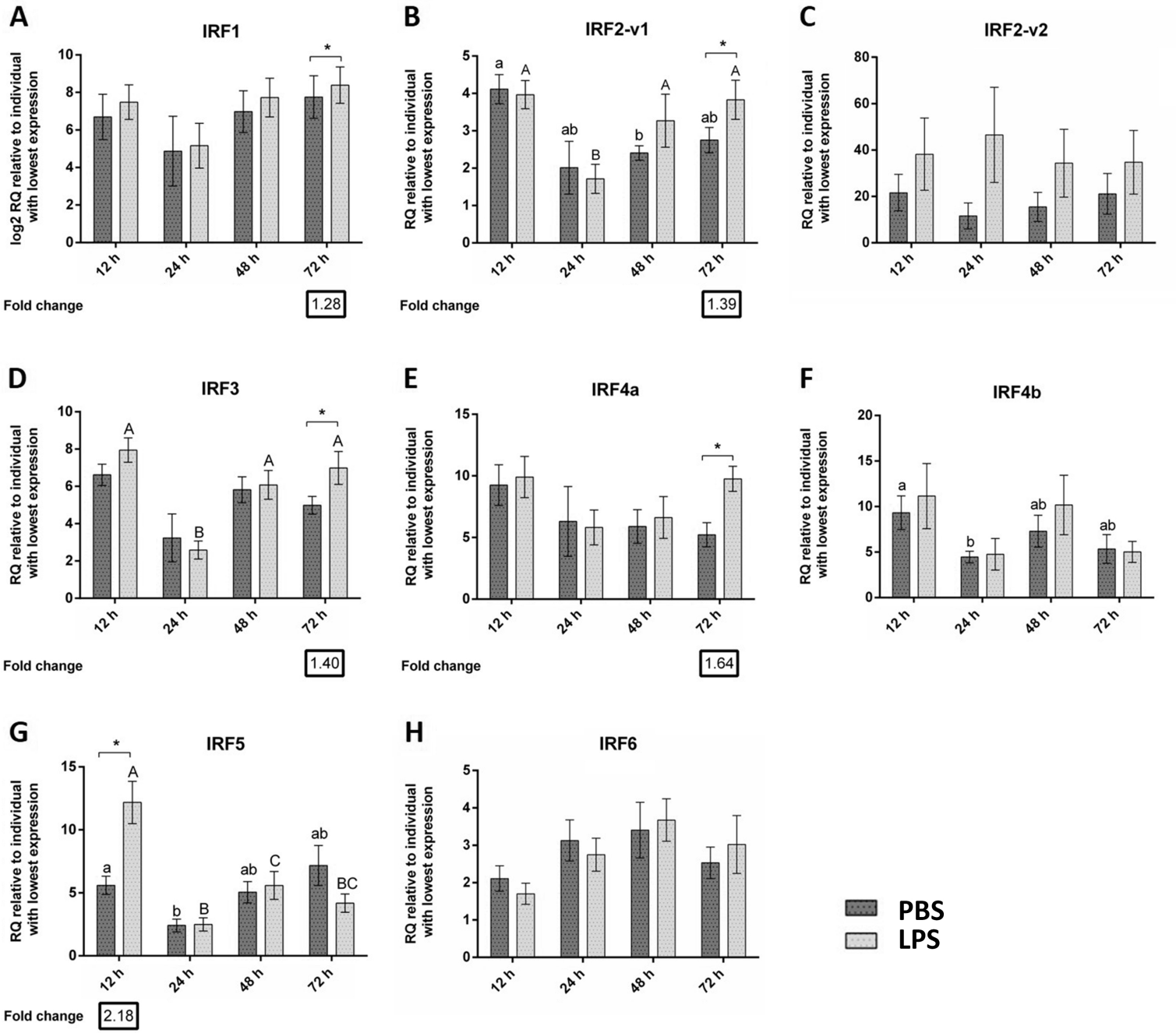
A
IRF1
log2 RQ relative to individual with lowest expression
12 h
24 h
48 h
72 h
*
Fold change
1.28
B
IRF2-v1
RQ relative to individual with lowest expression
a
A
ab
B
b
A
ab
A
*
Fold change
1.39
C
IRF2-v2
RQ relative to individual with lowest expression
D
IRF3
RQ relative to individual with lowest expression
A
B
A
*
A
Fold change
1.40
E
IRF4a
RQ relative to individual with lowest expression
*
Fold change
1.64
F
IRF4b
RQ relative to individual with lowest expression
a
b
ab
ab
G
IRF5
RQ relative to individual with lowest expression
*
a
A
b
B
ab
C
ab
BC
Fold change
2.18
H
IRF6
RQ relative to individual with lowest expression
PBS
LPS

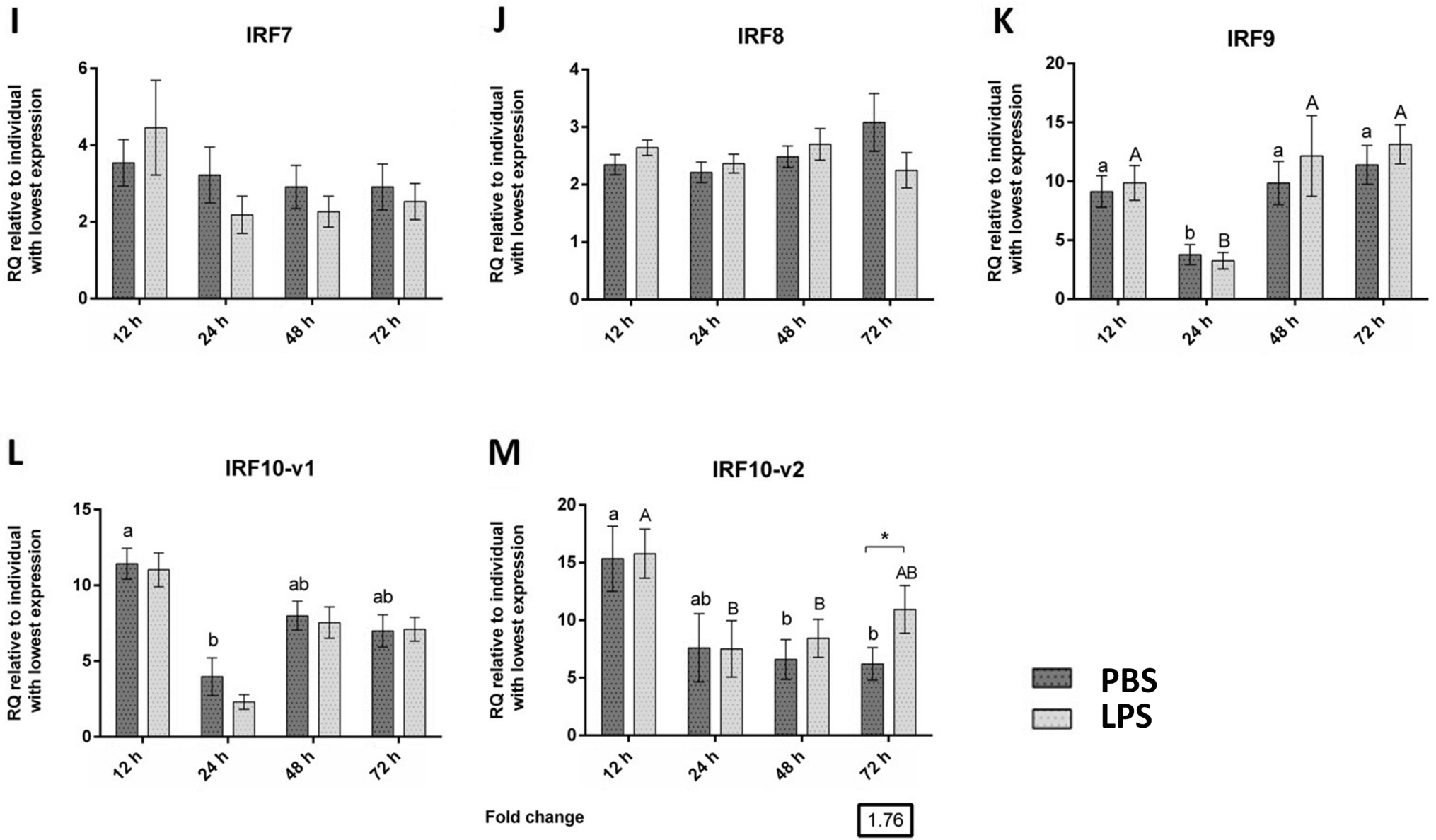
I
IRF7
RQ relative to individual with lowest expression
12 h
24 h
48 h
72 h
J
IRF8
K
IRF9
L
IRF10-v1
M
IRF10-v2
Fold change
1.76
PBS
LPS

Table 1: Primers used in RACE for characterization of Atlantic cod *Irf2*, *Irf3*, *Irf5*, *Irf6*, and *Irf9*

Primer name	Sequence (5'-3')	Amplicon length (bp)
Irf2-race-5'1	GGAGGAGCTGACCATCTGCTCTT	868
Irf2-race-5'2	GTACGAAGACACGGGAGAGATCTG	901
Irf2-race-3'1	CCCAATAGGCGAGCACCTGATCAC	575 / 792
Irf2-race-3'2	GCTGCCATTTGTCTGCCAGACCAT	543 / 759
Irf3-race-5'1	GCCCGAAGGGTGCTGCGGAAGT	327
Irf3-race-5'2	CACCTTGATGGGGTTGGCGTTTTC	373
Irf3-race-3'1	GTCAGTGTTCTACAGAGGGGTGAAG	889
Irf3-race-3'2	CTGGTGGATAACGAAGCTGGTTTC	853
Irf3-race-mid-f	CCCTCCGTCTGGAAGAGGAACTT	302
Irf3-race-mid-r	CGGTTCTGCACCGAGTCGAAGGT	
Irf5-race-5'1	GCCTCCGTGTAGAACCTCTGCTT	874
Irf5-race-5'2	CAGGATCAGCCCGCGGTCCATGA	912
Irf5-race-3'1	CTTGCTGAGCAGCCTCCCATTGAC	815
Irf5-race-3'2	GAAGTTCGAGTACCGCGGACGAA	789
Irf6-race-5'1	CTGCACCTCCAGGTCCGTCACTGA	908
Irf6-race-3'1	CAGCCCATCCCCCTGCTGGAGTT	972
Irf9-race-5'1	CAGGTCCCGCCGGGAGGAAGATG	996
Irf9-race-3'1	CTTCCACGTGGCGGTCAGCTACT	935

[1]Amplicon length was determined as the length of consensus sequence (obtained using Lasergene SeqMan Pro software – see Section 2.2), based on a minimum of six sequencing reads per amplicon.

Table 2: Primers used in RT-PCR and QPCR studies of Atlantic cod IRF family members

Primer name[1]	Sequence (5'-3')	Amplicon size (bp)	% Efficiency[2] (developmental/ macrophage)	Genomic location [linkage group (LG) gadMor2]
Irf1-fwd	AGAAGGACGCCAGTCTGTTCAA	101	89.1 / 91.8	LG 07
Irf1-rev	GCGGAAGTTGGCTTTCCATT			
Irf2-v1-fwd	CCAACCCGCTCATCAGTTAC	138	96.2 / 97.7	LG 10
Irf2-v1-rev	AGGTCAGAGGTCAGGACGAG			
Irf2-v2-fwd	TCCTCCCACTCCTACCCTCT	127	95.2 / 96.5	
Irf2-v2-rev	TTTGAATCGCTTGACAGCAC			
Irf3-fwd	TTCTGGAGCCGCTGTAAGTT	143	105.7 / 101.2	LG 18
Irf3-rev	AGACAGCAGGACGGACATTT			
Irf4a-fwd[a]	TGTACCGTATCATCCCAGAGG	111	101.3 / 103.8	LG 08
Irf4a-rev[a]	AGTGGGGTATCTGGCTGTGA			
Irf4b-fwd[a]	TGGACATCACCGAACCCTAC	106	91.3 / 90.3	LG 12
Irf4b-rev[a]	CATGACGAAAGCCATCTGAA			
Irf5-fwd	CTCTGCCAGTGCAAGGTGTA	143	94.6 / 95.1	LG 19
Irf5-rev	GAATCCCCCTTGTGGAACAT			
Irf6-fwd	GGAAGGTGAAGCTGTTCTGC	172	104.3 / 107.2	LG 13
Irf6-rev	ACCACCGGAATGATCTGAAC			
Irf7-fwd[a]	CATGTGCTTTGGGGAGAAGT	152	92.8 / 98.5	LG 09
Irf7-rev[a]	TCTGTAGGCTGACGTTGGTG			
Irf8-fwd[a]	TCGGGGAGGAACTACATGAC	158	90.7 / 91.1	LG 14
Irf8-rev[a]	GGCCATCTCGTCTGACATCT			
Irf9-fwd	GAGACGCCCAACAAGATCC	179	87.3 / 88.5	LG 23
Irf9-rev	AGGATGAGCTTCTGGGACTG			
Irf10-v1-fwd[a]	CCGAGAAGCCCAATAAACTG	143	97.0 / 99.3	LG 01
Irf10-v1-rev[a]	ATACTCCTCGCCAAAGCAGA			
Irf10-v2-fwd[a]	GGTCCAACGCAGTAACGATT	134	96.9 / 98.3	
Irf10-v2-rev[a]	ACTGTGGGAGACTGGCGTAT			
EF1α-fwd[a]	CCCTCCAGGACGTCTACAAG	150	88.5 / N/A	N/A
EF1α-rev[a]	GAGACTCGTGGTGCATCTCA			
Tubb2-fwd	GACCCCACAGGAAGCTACAA	129	N/A / 89.8	N/A
Tubb2-rev	CATAGTGCCAGGCTCCAAGT			
EIF3-fwd[b]	AACTGTCCGTAGTCCGCAAG	125	N/A / 94.3	N/A
EIF3-rev[b]	CTGCTCAGCGAGAAACAGAA			
rplp1-fwd[b]	TCTGAAGCTAAGGCCCTCAA	141	92.5 / N/A	N/A
rplp1-rev[b]	ATCGTCGTGGAGGATCAGAG			

[1] Primers noted with "a" were designed and first used in our previous study (Inkpen *et al*., 2015); primers noted with "b" were previously used in Eslamloo *et al*. (2016).

[2] Percent amplification efficiency as in Pfaffl (2001) calculated using 7500 Fast software (Applied Biosystems).

Table 3: Summary of IRF transcript expression responses to immune stimulation in Atlantic cod

Transcript	Macrophage response to poly(I:C), current study	Response to virus / viral PAMPs (previous studies)	Macrophage response to LPS, current study	Response to bacteria / bacterial PAMPs (previous studies)
GmIrf1	Upregulated (12, 48 HPS).	Upregulated by poly(I:C) in spleen (Rise *et al*., 2008; Hori *et al*., 2012). Upregulated by nervous necrosis virus (NNV) in brain (Krasnov *et al*., 2013)	Upregulated only at 72 HPS.	Upregulated by killed atypical *Aeromonas salmonicida* in spleen, head kidney (Feng *et al*., 2009).
GmIrf2-v1	Upregulated (all time-points)	Upregulated by NNV in brain (Krasnov *et al*., 2013).	Upregulated only at 72 HPS.	No previous studies.
GmIrf2-v2	Upregulated only at 24 HPS.	No previous studies.	No significant response.	
GmIrf3	Upregulated (all time-points).	Upregulated by poly(I:C) in larval cells; upregulated by NNV in brain (Krasnov *et al*., 2013).	Upregulated only at 72 HPS.	No previous studies.
GmIrf4a	Upregulated (all time-points).	Downregulated by poly(I:C) (Inkpen *et al*., 2015).	Upregulated only at 72 HPS.	No response to ASAL in spleen (Inkpen *et al*., 2015).
GmIrf4b	Upregulated (all time-points).	Upregulated by poly(I:C) in spleen (Inkpen *et al*., 2015).	No significant response.	Upregulated by ASAL in spleen (Inkpen *et al*., 2015).
GmIrf5	Upregulated (12-24 HPS).	No previous studies.	Upregulated only at 12 HPS.	No previous studies.
GmIrf6	No significant response.	No previous studies.	No significant response.	No previous studies.
GmIrf7	Upregulated (12-48 HPS).	Upregulated by poly(I:C) in spleen (Rise *et al*., 2008; Hori *et al*., 2012). Upregulated by poly(I:C) in larval cells; upregulated by NNV in brain (Krasnov *et al*., 2013).	No significant response.	Upregulated by ASAL in spleen (Inkpen *et al*., 2015).
GmIrf8	No significant response.	Upregulated by poly(I:C) in spleen (Inkpen *et al*., 2015).	No significant response.	Downregulated, then upregulated by ASAL in spleen (Inkpen *et al*., 2015).
GmIrf9	Upregulated (all time-points).	Upregulated by NNV in brain (Krasnov *et al*., 2013).	No significant response.	No previous studies.
GmIrf10-v1	Upregulated (all time-points).	Upregulated by poly(I:C) in spleen (Inkpen *et al*., 2015). Upregulated by poly(I:C) in larval cells (Krasnov *et al*., 2013).	No significant response.	Upregulated by ASAL in spleen (Inkpen *et al*., 2015).
GmIrf10-v2	Upregulated (48-72 HPS).	No previous studies.	Upregulated only at 72 HPS.	No previous studies.

Supplemental Figure 1: Representative images of Atlantic cod embryos and larvae sampled from 0 to 17 days post fertilization. Size bar = 1 mm. Embryos at 0 dpf (A) were observed to have some variation in stage, but most were at the 64 to 128 cell stage. Gastrulation was observed to be complete at 5 dpf (F). Hatching began at 13 dpf (N) and was complete at 15 dpf (P). Determination of developmental stages was based on descriptions by Hall *et al*. (2004).

Supplemental Figure 2: Nucleotide sequence of *Irf2-v1* cDNA and inferred amino acid translation. (GenBank accession MH813456). Nucleotide sequence is numbered on the left, while the predicted amino acid sequence is numbered on the right. The open reading frame is shown in upper case letters while 5' and 3' untranslated regions are in lower case letters. Nucleotide sequence of the DNA binding domain is shaded in grey. Locations of predicted introns are indicated based on gadMor2 genome assembly. The stop codon is marked with an asterisk (*). A putative polyadenylation signal is underlined.

Supplemental Figure 3: Nucleotide sequence of *Irf2-v2* cDNA and inferred amino acid translation. (GenBank accession MH813457). Nucleotide sequence is numbered on the left, while the predicted amino acid sequence is numbered on the right. The open reading frame is shown in upper case letters while 5' and 3' untranslated regions are in lower case letters. Nucleotide sequence of the DNA binding domain is shaded in grey. Locations of predicted introns are indicated based on gadMor2 genome assembly. The stop codon is marked with an

asterisk (*). Two possible polyadenylation signals are underlined. (The use of polyadenylation signals other than AAUAAA is discussed in [1]MacDonald and Rodando, 2002).

Supplemental Figure 4: Nucleotide sequence of *Irf3* cDNA and inferred amino acid translation. (GenBank accession MH813458). Nucleotide sequence is numbered on the left, while the predicted amino acid sequence is numbered on the right. The open reading frame is shown in upper case letters while 5' and 3' untranslated regions are in lower case letters. Nucleotide sequence of the DNA binding domain is shaded in grey. Locations of predicted introns are indicated based on gadMor2 genome assembly. The stop codon is marked with an asterisk (*).

Supplemental Figure 5: Nucleotide sequence of *Irf5* cDNA and inferred amino acid translation. (GenBank accession MH813459). Nucleotide sequence is numbered on the left, while the predicted amino acid sequence is numbered on the right. The open reading frame is shown in upper case letters while 5' and 3' untranslated regions are in lower case letters. Nucleotide sequence of the DNA binding domain is shaded in grey. Locations of predicted introns are indicated based on gadMor2 genome assembly. The stop codon is marked with an asterisk (*).

Supplemental Figure 6: Nucleotide sequence of *Irf6* cDNA and inferred amino acid translation. (GenBank accession MH813460). Nucleotide sequence is numbered on the left,

while the predicted amino acid sequence is numbered on the right. The open reading frame is shown in upper case letters while 5' and 3' untranslated regions are in lower case letters. Nucleotide sequence of the DNA binding domain is shaded in grey. Locations of predicted introns are indicated based on gadMor2 genome assembly. The stop codon is marked with an asterisk (*). A putative polyadenylation signal is underlined.

Supplemental Figure 7: Nucleotide sequence of *Irf9* cDNA and inferred amino acid translation. (GenBank accession MH813461). Nucleotide sequence is numbered on the left, while the predicted amino acid sequence is numbered on the right. The open reading frame is shown in upper case letters while 5' and 3' untranslated regions are in lower case letters. Nucleotide sequence of the DNA binding domain is shaded in grey. Locations of predicted introns are indicated based on gadMor2 genome assembly. The stop codon is marked with an asterisk (*). A putative polyadenylation signal is underlined.

Supplemental Figure 8: Multiple sequence alignments of Atlantic cod IRF protein sequences. Sequences were retrieved from the NCBI non-redundant protein database (see Supplemental Table 1). Alignments were carried out using the ClustalW algorithm in MEGA7 software (Kumar *et al*., 2016). Identical amino acids are indicated by asterisks (*); conservative substitutions are indicated by colons (:). Conserved tryptophan (W) residues are boxed.

A) Alignment of predicted cod IRF DBD sequences with homologous sequences from other teleost fish. IRF family subgroups are noted along the right side**. B) Alignment of predicted**

full length cod IRF sequences. DNA binding domain and IRF-associated domain are shaded in grey. Truncated splice variants (IRF2-v2, IRF10-v2) are omitted.

Supplemental Figure 9: Composite agarose gel image of IRF transcript expression in 18 Atlantic cod tissues. All gels are 1.7% agarose in TAE buffer. PCR was carried out using samples from two fish. Bl=blood, Ey=eye, Br=brain, Gi=gill, Hr=heart, HK=hematopoietic (head) kidney, PK=posterior (trunk) kidney, Sp=spleen, Li=liver, Go=gonad, St=stomach, PC=pyloric caecum, Mg=midgut, Hg=hindgut, DS=dorsal skin, VS=ventral skin, Mu=skeletal muscle, Fn=fin, C=no-template control.

Supplemental Figure 10: Atlantic cod macrophage transcript expression response of antiviral and antibacterial biomarkers to (A) poly(I:C) and (B) LPS, measured by QPCR. Data is presented as mean +/- SEM, normalized to the geometric mean of *EF1α* and *rplp1* expression, with the lowest expressing sample set to RQ=1. An asterisk (*) represents a significant difference between a poly(I:C) or LPS stimulated group and the time-matched PBS group ($p < 0.05$). [** = $p<0.01$; *** = $p<0.001$; **** = $p<0.0001$]. Capital letters and lower case letters represent similarity among PBS-treated groups and poly(I:C)/LPS-treated groups across time points, respectively. Fold change is calculated as (mean poly(I:C) or LPS)/(mean PBS).

[1]MacDonald CC, Redondo JL. 2002. Reexamining the polyadenylation signal: were we wrong about AAUAAA? Mol Cell Endocrinol 190(1-2):1-8.

Supplemental Figure 1

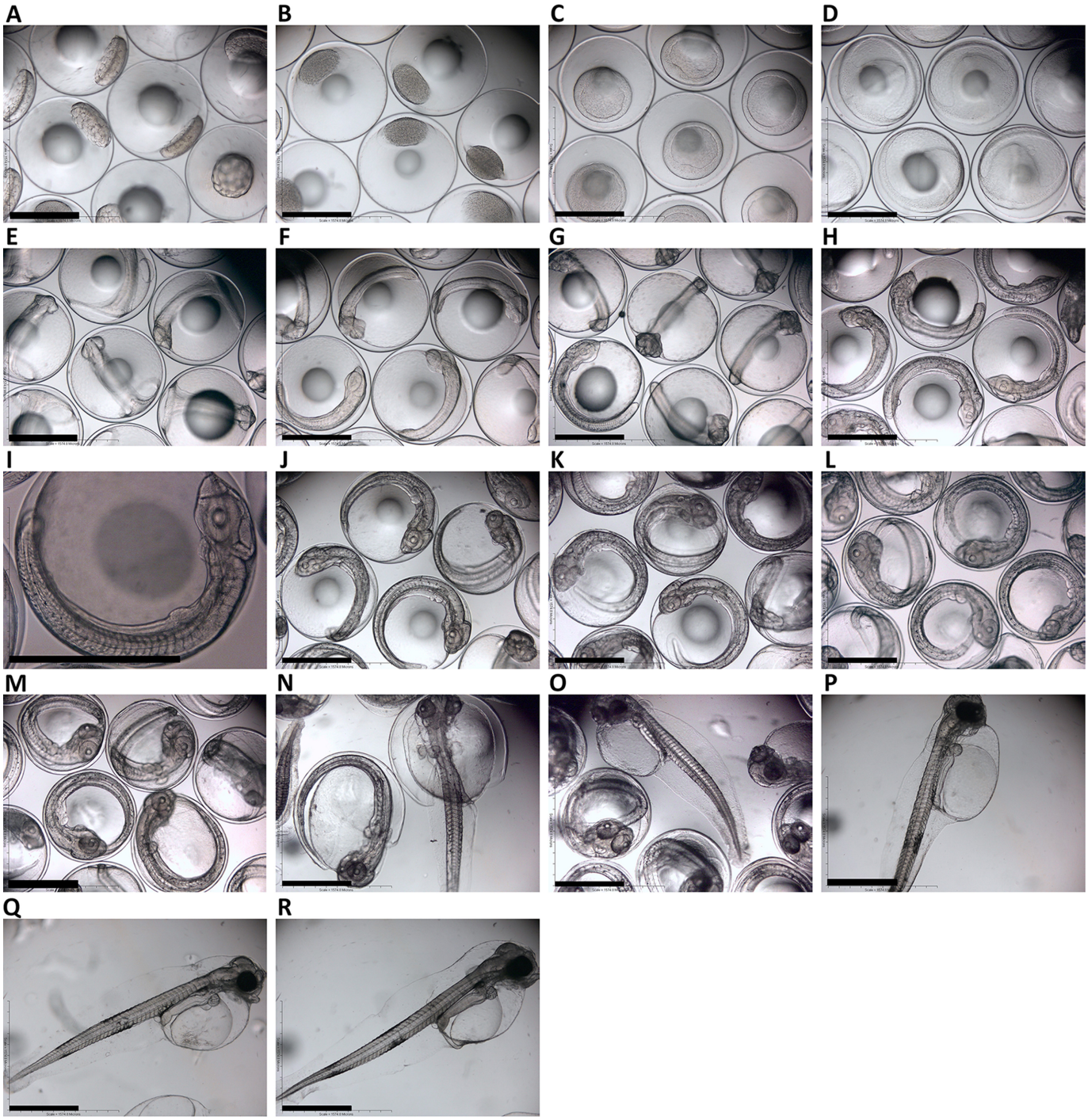

Supplemental Figure 2

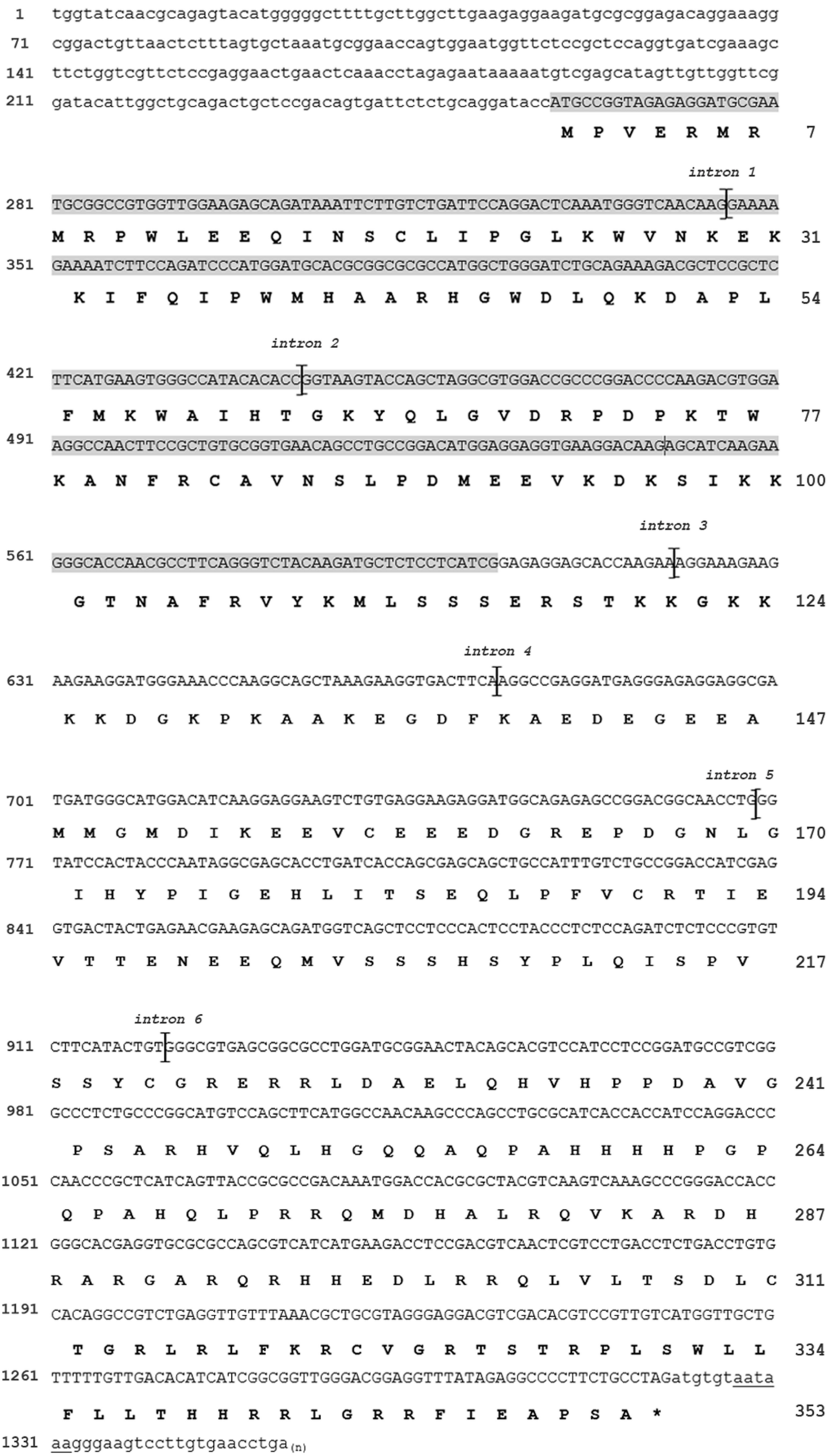

Supplemental Figure 3

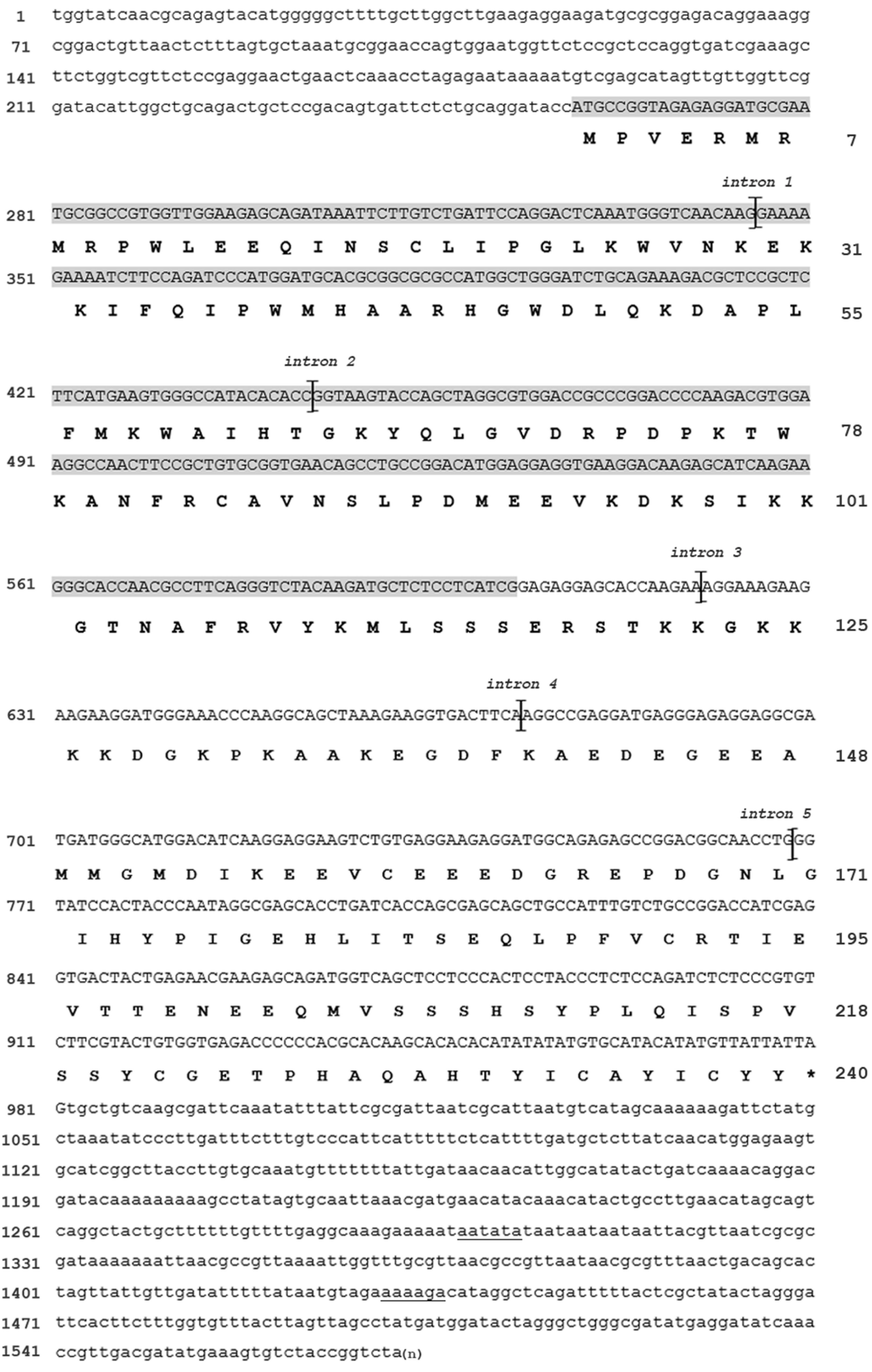

Supplemental Figure 4

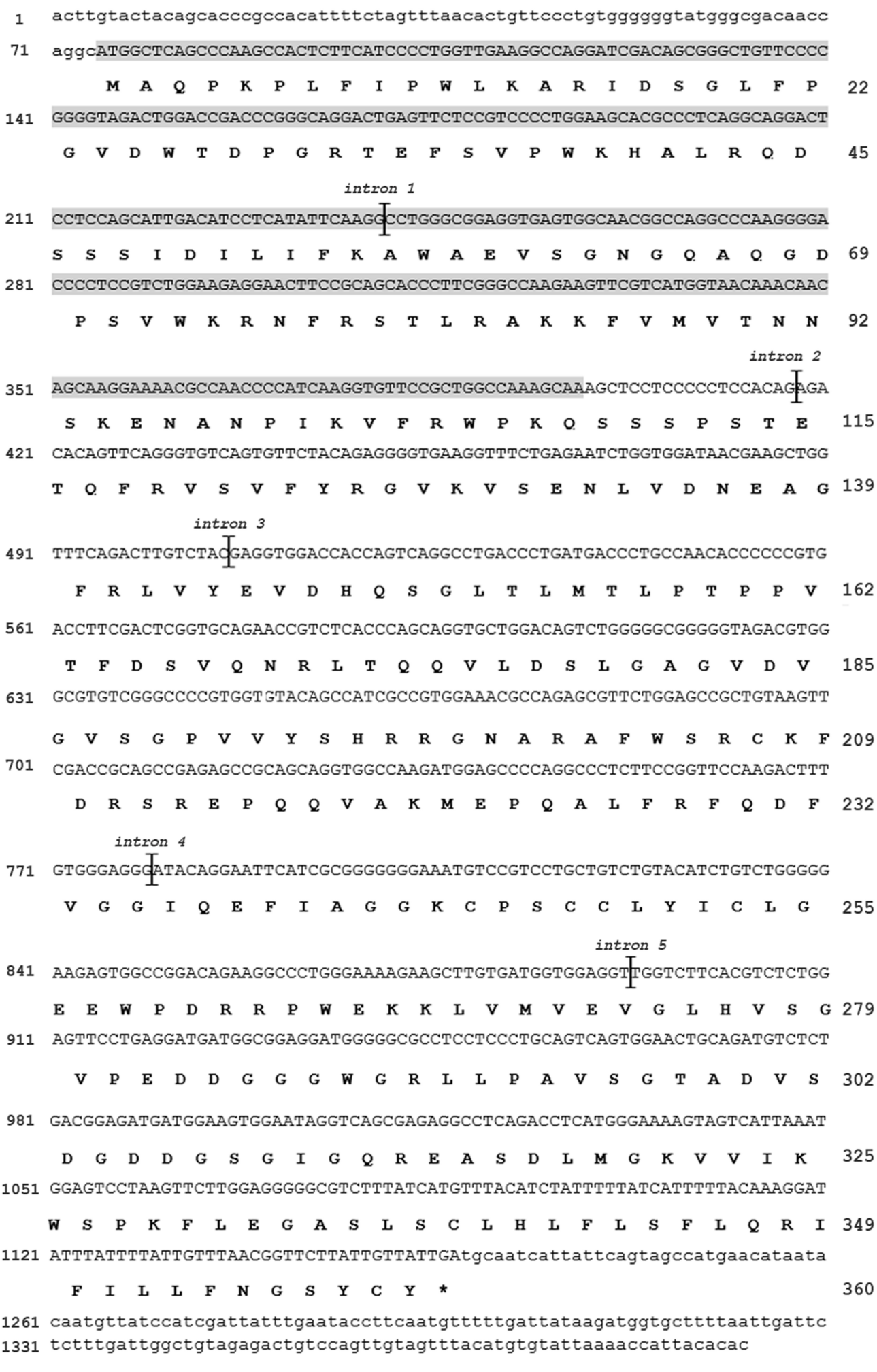

Supplemental Figure 5

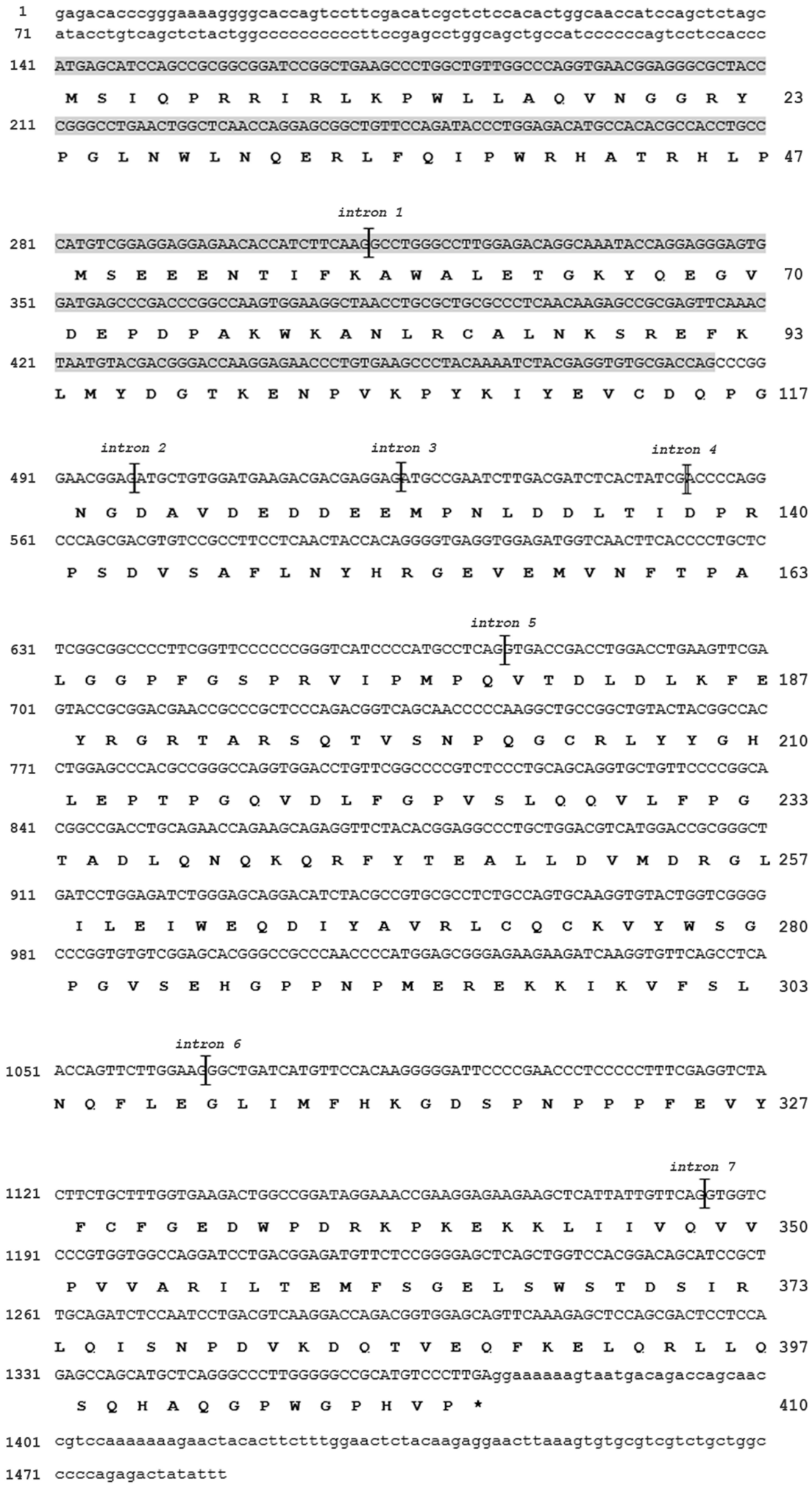

Supplemental Figure 6

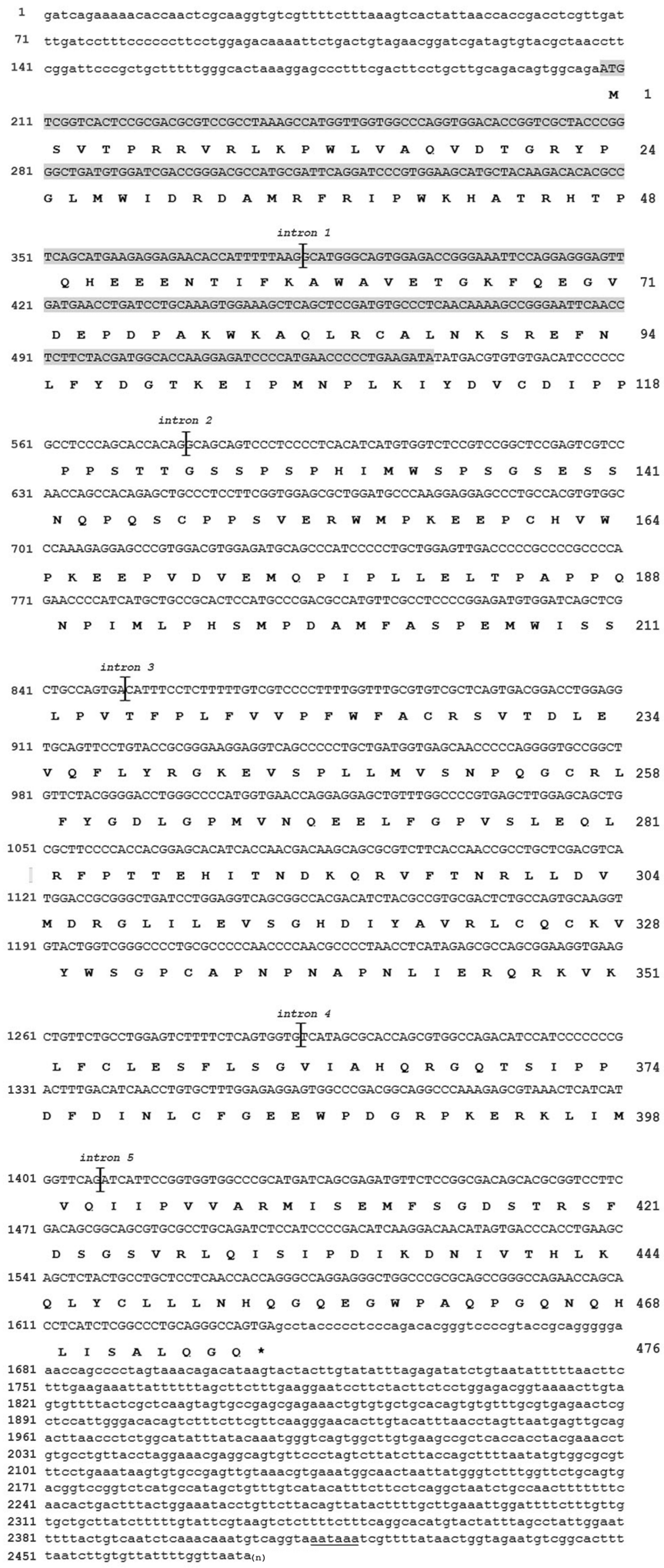

Supplemental Figure 7

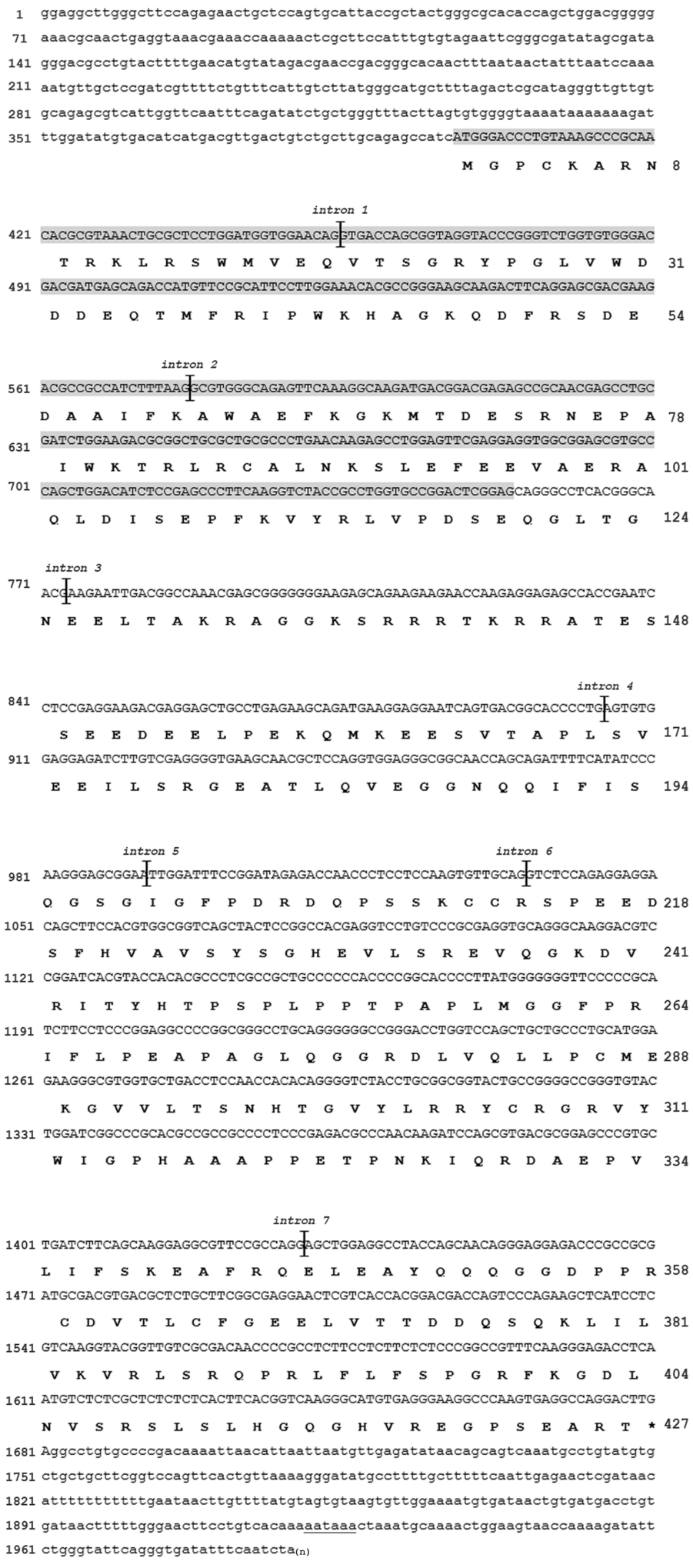

Supplemental Figure 8

A

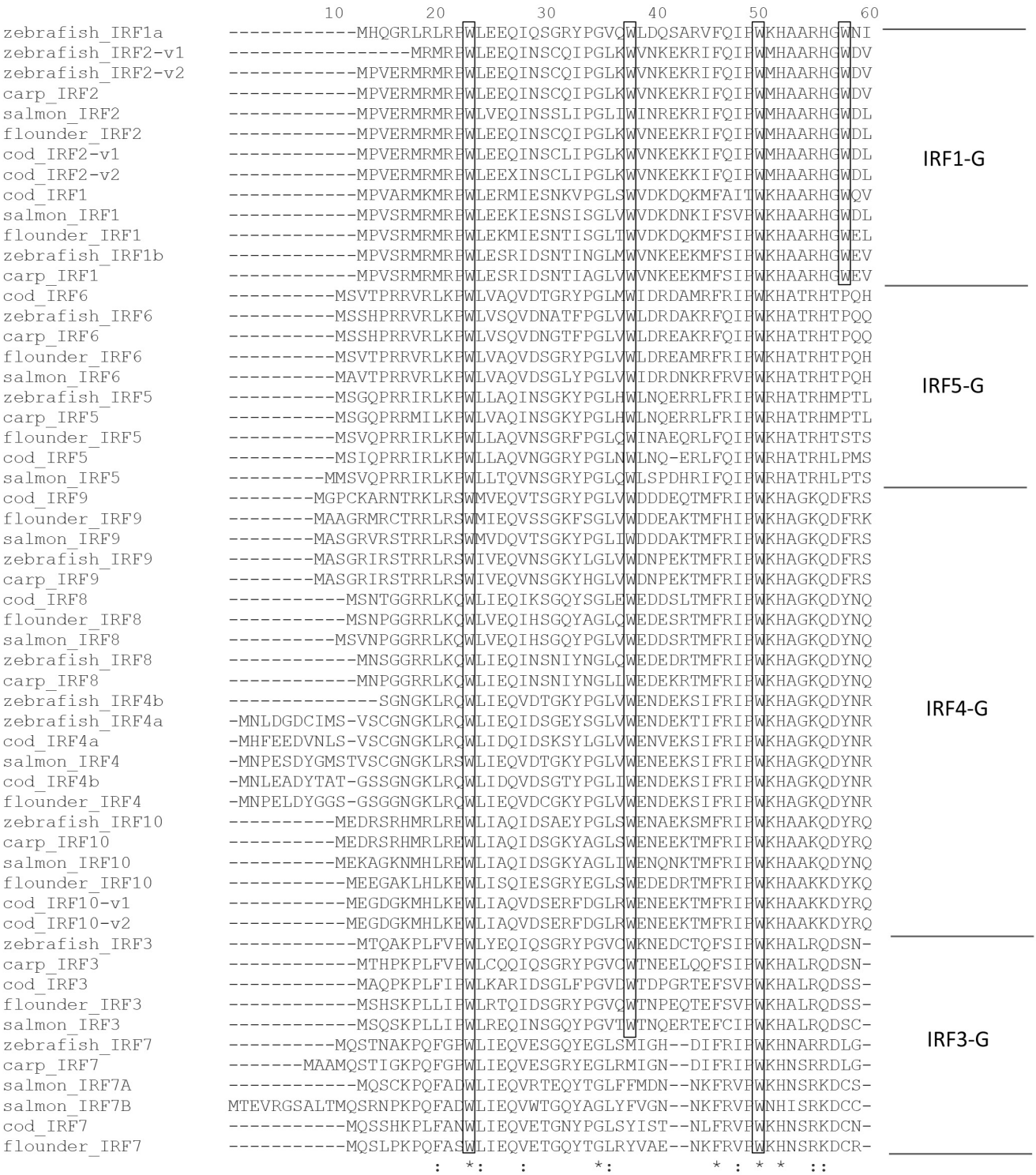

Supplemental Figure 8

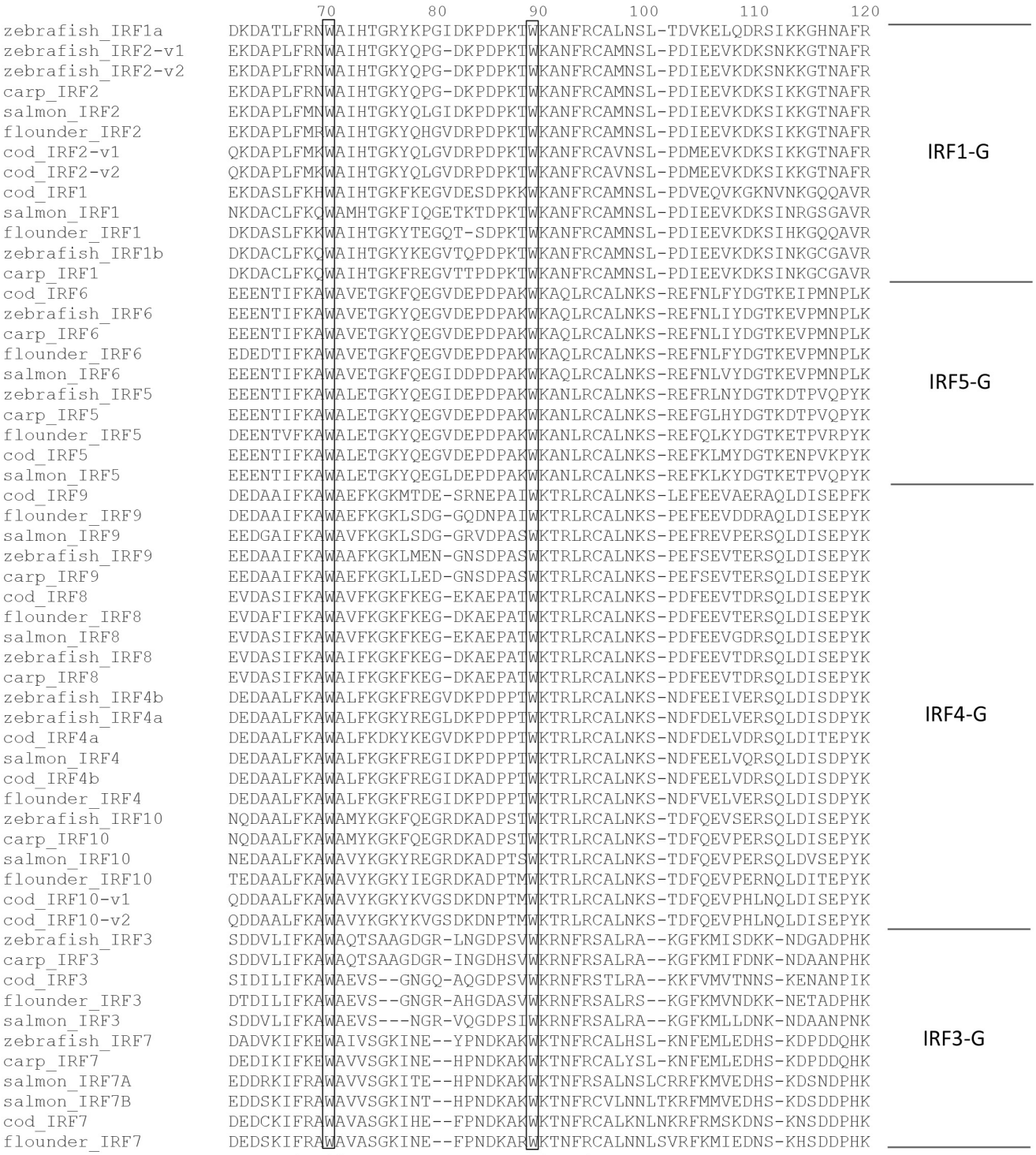

Supplemental Figure 8

B

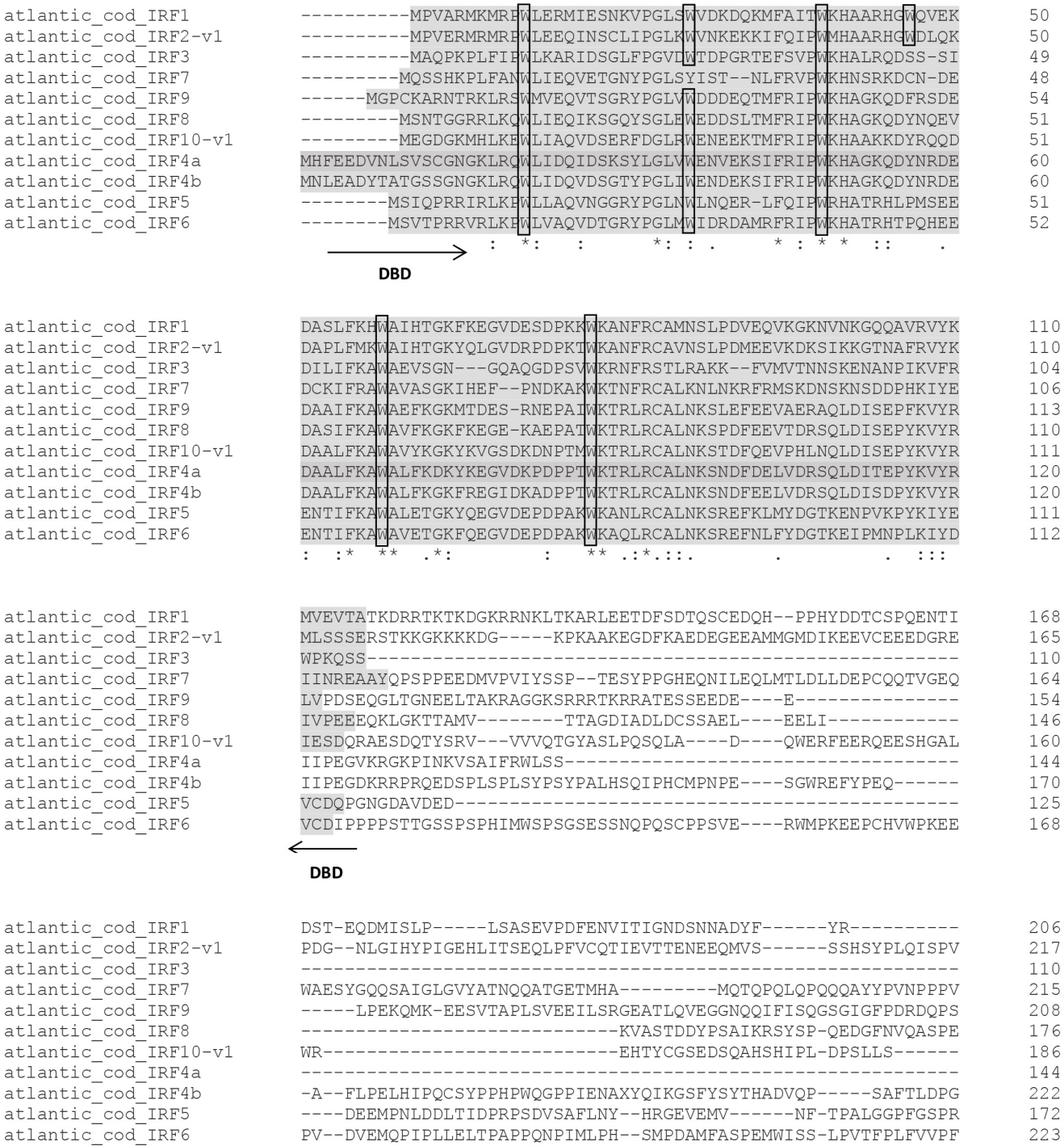

Supplemental Figure 8

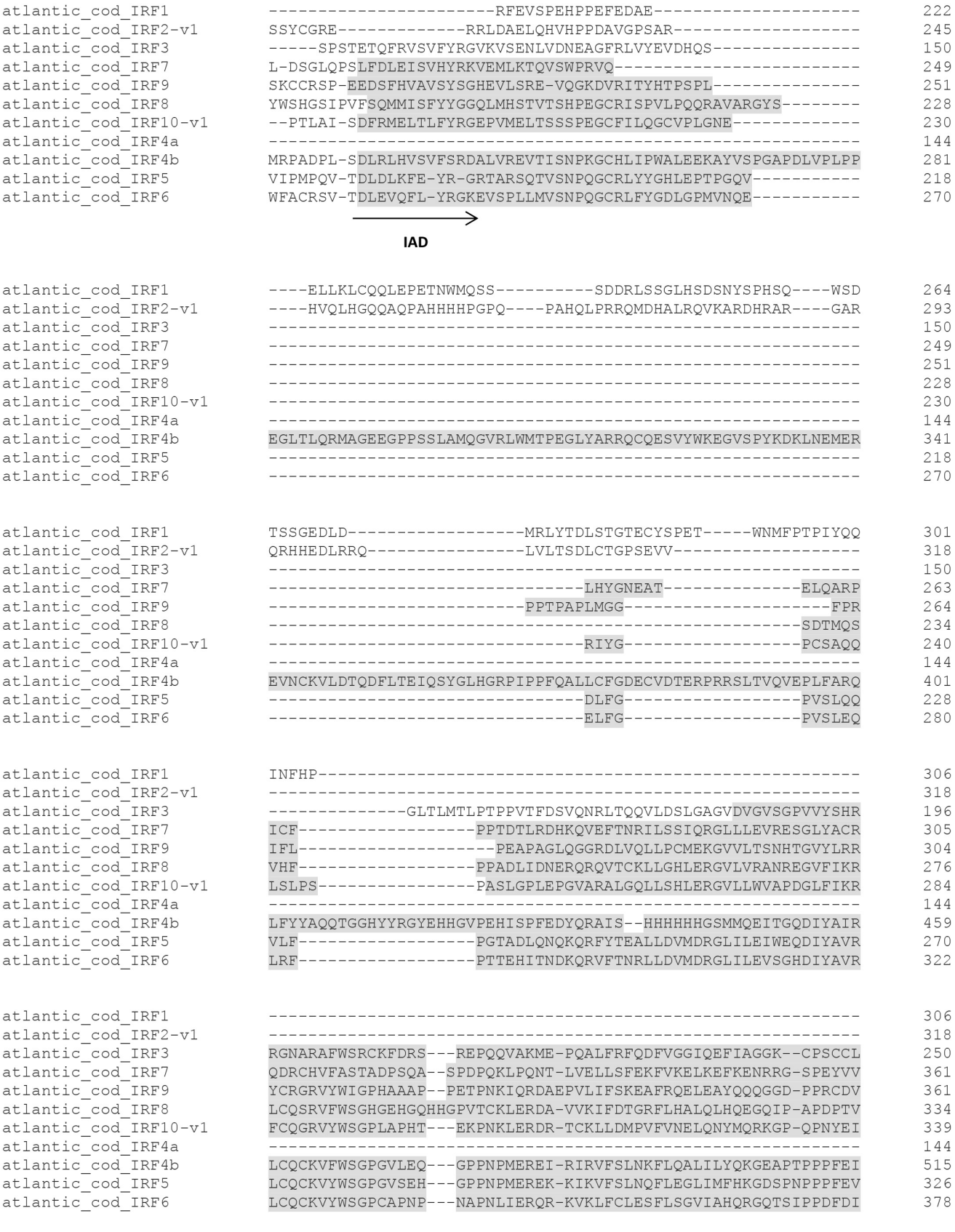

Supplemental Figure 8

```
atlantic_cod_IRF1        ------------------------------------------------------------  306
atlantic_cod_IRF2-v1     ------------------------------------------------------------  318
atlantic_cod_IRF3        YICLGEEWPDRRP-WEKKLVMVEVGLHVSGVP-----EDDGGG------WGRLLPAVSGT  298
atlantic_cod_IRF7        NMCFGEKFPDGKP-LEKKLIVVKVVPLICRYF----YEMAQVEGASSLDSTNVSLQISHD  416
atlantic_cod_IRF9        TLCFGEELVTTDD-QSQKLILVKVRLSRQPRLFLFSPGRFKGDLNVSRS-----LSLHGQ  415
atlantic_cod_IRF8        TLCFGEELHDLSN-AKNKLILVQITAMNCQQL----LEAVNMRAVQSYNHS---PSVEMS  386
atlantic_cod_IRF10-v1    DLCFGEEYPDAKVSKTMKLITVHVVPLFAMEL----LQRFQLERVEAEP------DVHTP  389
atlantic_cod_IRF4a       ------------------------------------------------------------  144
atlantic_cod_IRF4b       YFCFGEDWPDRKP-KEKKLIIVQVVPVVARIL----TEMFSGEL--SWSTDSIRLQISNP  568
atlantic_cod_IRF5        YFCFGEDWPDRKP-KEKKLIIVQVVPVVARIL----TEMFSGEL--SWSTDSIRLQISNP  379
atlantic_cod_IRF6        NLCFGEEWPDGRP-KERKLIMVQIIPVVARMI----SEMFSGDSTRSFDSGSVRLQISIP  433


atlantic_cod_IRF1        ------------------------------------------------------------  306
atlantic_cod_IRF2-v1     ------------------------------------------------------------  318
atlantic_cod_IRF3        ADVSDGDDGSGIGQREASDLMG-----KVVIKWSPKFLEGASLSCLHLFLSFLQRIFILL  353
atlantic_cod_IRF7        S-----LY---DLISSAFGLPGSQVAPQLVGHY--------------------------  441
atlantic_cod_IRF9        GHVREGPS---EART---------------------------------------------  427
atlantic_cod_IRF8        DEMAS------DQMARIYQDLCSYSAPQRTDCYRDNMTITA--------------------  421
atlantic_cod_IRF10-v1    KEAKDEM-----------------------------------------------------  396
atlantic_cod_IRF4a       ------------------------------------------------------------  144
atlantic_cod_IRF4b       D-LKDHTV---EQFKEIHRLLQSQSA---HPNWPTN----------------------  597
atlantic_cod_IRF5        D-VKDQTV---EQFKELQRLLQSQHA---QGPWGPHVP--------------------  410
atlantic_cod_IRF6        D-IKDNIV---THLKQLYCLLLNHQG---QEGWPAQPGQNQHLISALQGQ----------  476
```

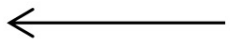

IAD

Supplemental Figure 9

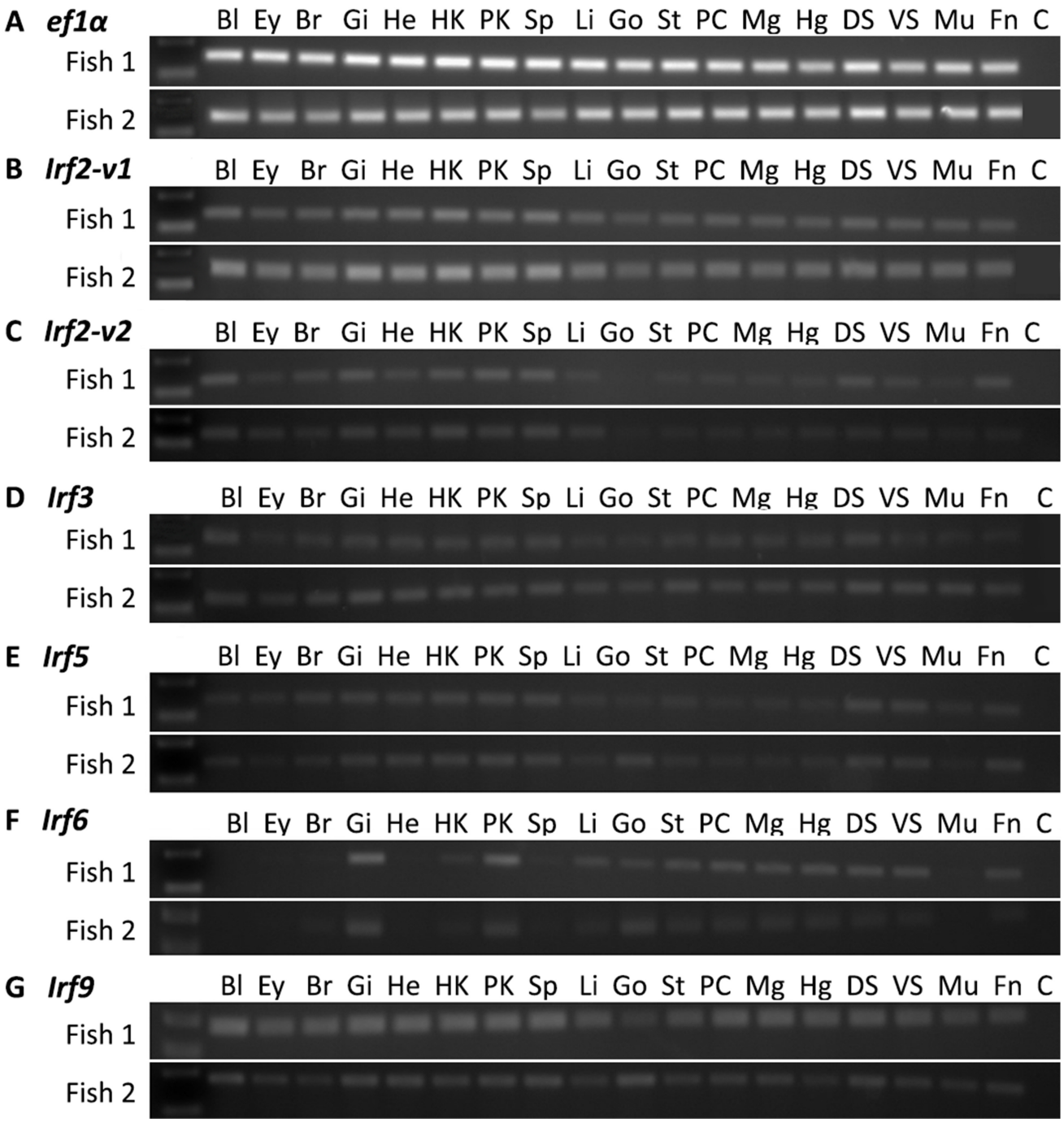

A

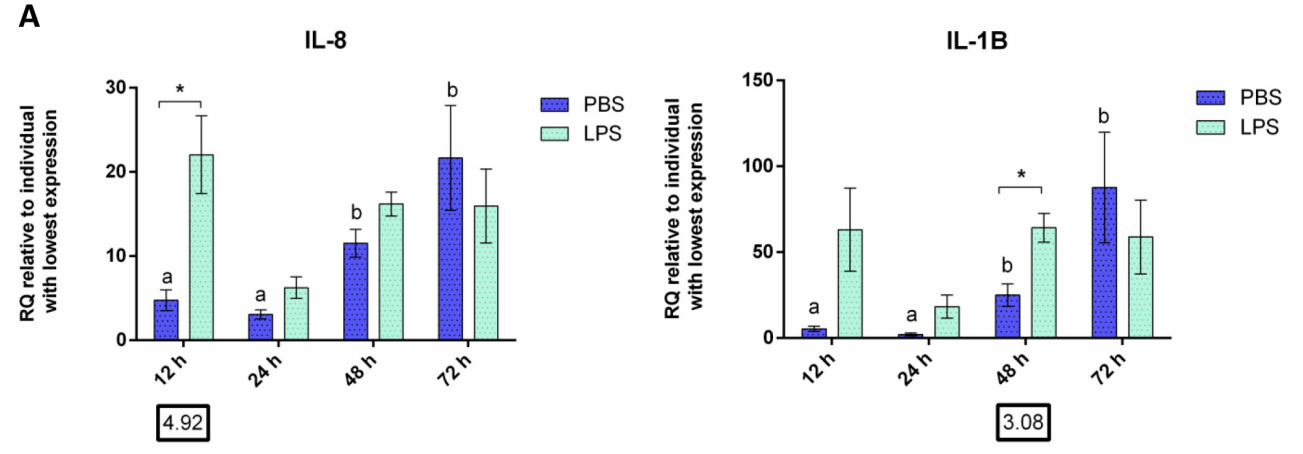
IL-8
RQ relative to individual with lowest expression
PBS
LPS
12 h
24 h
48 h
72 h
4.92
IL-1B
3.08

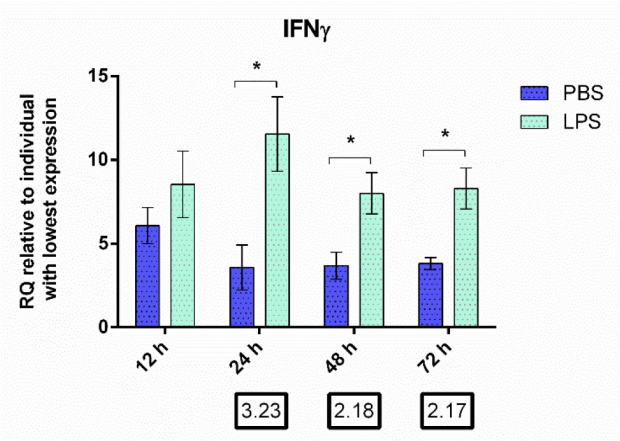
IFNγ
RQ relative to individual with lowest expression
PBS
LPS
3.23
2.18
2.17

B

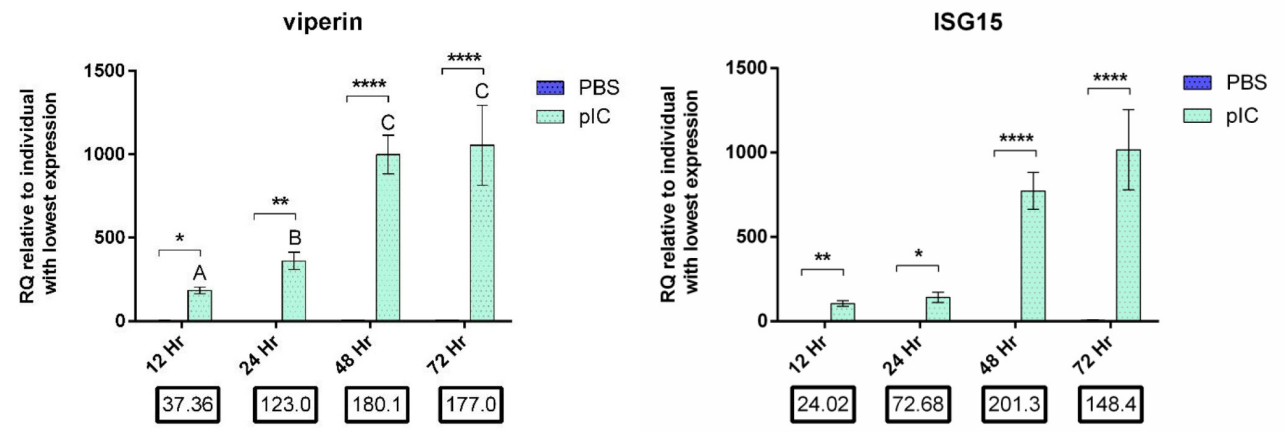
viperin
RQ relative to individual with lowest expression
PBS
pIC
12 Hr
24 Hr
48 Hr
72 Hr
37.36
123.0
180.1
177.0
ISG15
24.02
72.68
201.3
148.4

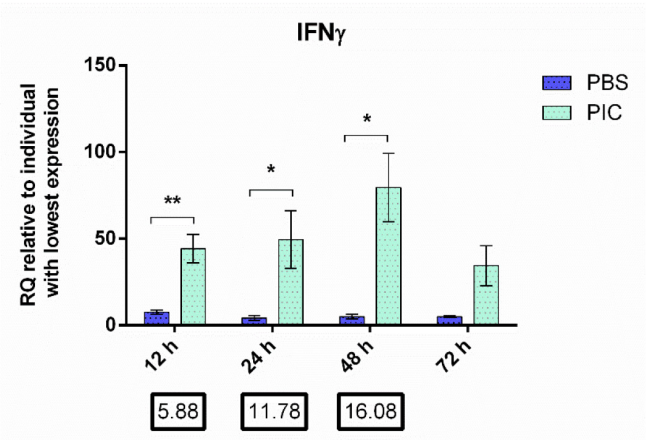
IFNγ
RQ relative to individual with lowest expression
PBS
PIC
12 h
24 h
48 h
72 h
5.88
11.78
16.08

Supplemental Table 1: Teleost fish IRF amino acid sequences used in phylogenetic analysis

Protein name	Species name (common name)	GenBank accession no.
IRF1	*Ctenopharyngodon idella* (grass carp)	ADF57571
	Gadus morhua (Atlantic cod)	ADG85733
	Oncorhynchus mykiss (rainbow trout)	AAM77843
	Paralichthys olivaceus (Japanese flounder)	BAA83468
	Salmo salar (Atlantic salmon)	ACI68339
	Tetraodon nigroviridis (pufferfish)	CAF87280
IRF1a	*Danio rerio* (zebrafish)	AAI15341
IRF1b[1]		AAH85555
IRF2	*Ctenopharyngodon idella* (grass carp)	AFV99156
	Danio rerio (zebrafish)	AAI64907
	Gadus morhua (Atlantic cod)	**MH813456 (v1)**
	Oncorhynchus mykiss (rainbow trout)	AAK53987
	Paralichthys olivaceus (Japanese flounder)	ADZ96216
	Salmo salar (Atlantic salmon)	ACI33066
IRF3	*Ctenopharyngodon idella* (grass carp)	AHL29306
	Danio rerio (zebrafish)	ABY91288
	Gadus morhua (Atlantic cod)	**MH813458**
	Oncorhynchus mykiss (rainbow trout)	CAH56618
	Paralichthys olivaceus (Japanese flounder)	ACY69212
	Salmo salar (Atlantic salmon)	ACN11005
	Tetraodon nigroviridis (pufferfish)	CAG07572
IRF4	*Ctenopharyngodon idella* (grass carp)	AMT92193
	Oncorhynchus mykiss (rainbow trout)	CAH56622
	Paralichthys olivaceus (Japanese flounder)	AEY55358
	Salmo salar (Atlantic salmon)	ACI33264
	Tetraodon nigroviridis (pufferfish)	CAF98086
IRF4a	*Danio rerio* (zebrafish)	NP_001116182
	Gadus morhua (Atlantic cod)	AJR33027
IRF4b	*Danio rerio* (zebrafish)	CAI11951
	Gadus morhua (Atlantic cod)	AJR33026
IRF5	*Ctenopharyngodon idella* (grass carp)	ACT83675
	Danio rerio (zebrafish)	ABY91289
	Gadus morhua (Atlantic cod)	**MH813459**
	Oncorhynchus mykiss (rainbow trout)	CDQ64449
	Paralichthys olivaceus (Japanese flounder)	AEY55357
	Salmo salar (Atlantic salmon)	ACI33029
	Tetraodon nigroviridis (pufferfish)	CAF90666
IRF6	*Ctenopharyngodon idella* (grass carp)	AMT92196
	Danio rerio (zebrafish)	AAH56772
	Gadus morhua (Atlantic cod)	**MH813460**
	Oncorhynchus mykiss (rainbow trout)	CDQ66830
	Paralichthys olivaceus (Japanese flounder)	XP_019942637
	Salmo salar (Atlantic salmon)	XP_013988514
	Tetraodon nigroviridis (pufferfish)	CAG06823
IRF7	*Ctenopharyngodon idella* (grass carp)	ACS34986
	Danio rerio (zebrafish)	NP_956971

	Gadus morhua (Atlantic cod)	AJR33028
	Oncorhynchus mykiss (rainbow trout)	CAH56623
	Paralichthys olivaceus (Japanese flounder)	ACY69214
	Tetraodon nigroviridis (pufferfish)	CAG02387
IRF7A	*Salmo salar* (Atlantic salmon)	ACI33478
IRF7B		ACL68545
IRF8	*Ctenopharyngodon idella* (grass carp)	AMT92197
	Danio rerio (zebrafish)	AAH75963
	Gadus morhua (Atlantic cod)	AJR33029
	Oncorhynchus mykiss (rainbow trout)	ALS92677
	Paralichthys olivaceus (Japanese flounder)	AFE18694
	Salmo salar (Atlantic salmon)	XP_013982533
	Tetraodon nigroviridis (pufferfish)	CAF99526
IRF9	*Ctenopharyngodon idella* (grass carp)	AMT92198
	Danio rerio (zebrafish)	AAH81591
	Gadus morhua (Atlantic cod)	**MH813461**
	Oncorhynchus mykiss (rainbow trout)	CDQ76373
	Paralichthys olivaceus (Japanese flounder)	AHV91018
	Salmo salar (Atlantic salmon)	ACN11040
	Tetraodon nigroviridis (pufferfish)	AFR24260
IRF10	*Ctenopharyngodon idella* (grass carp)	ACT83676
	Danio rerio (zebrafish)	NP_998044
	Gadus morhua (Atlantic cod)	AJR33030 (v1)
	Paralichthys olivaceus (Japanese flounder)	BAI63219
	Salmo salar (Atlantic salmon)	XP_014000943
	Tetraodon nigroviridis (pufferfish)	CAG04088
IRF10a	*Oncorhynchus mykiss* (rainbow trout)	CDM74110
IRF10b		CDM74111

[1]Zebrafish IRF1b is also called IRF11.

*Bolded accession numbers represent **nucleotide** sequences characterized in the current study, as amino acid sequences are not yet available.

Supplemental Table 2: Normalizer transcript Ct values for early development and macrophage QPCR studies in Atlantic cod

Embryonic / larval QPCR normalizer Ct[1] values					Macrophage QPCR normalizer Ct values			
Sample Name[2]	***Tubb2***	***EIF3***	**Geometric mean**		**Sample Name[3]**	***EF1α***	***rplp1***	**Geometric mean**
D00T1	26.190	26.125	26.157		A12C	18.419	19.033	18.724
D00T2	25.596	26.086	25.840		B12C	18.055	18.075	18.065
D00T3	27.651	24.975	26.279		C12C	17.909	17.989	17.949
D01T1	24.720	25.866	25.286		D12C	18.159	18.304	18.231
D01T2	24.911	25.558	25.233		E12C	18.408	18.475	18.441
D01T3	26.317	24.809	25.552		F12C	18.116	18.205	18.160
D02T1	22.691	25.565	24.085		A12P	18.449	18.949	18.697
D02T2	22.761	25.278	23.986		B12P	18.628	18.107	18.366
D02T3	24.514	24.098	24.305		C12P	18.781	18.473	18.626
D03T1	21.230	24.347	22.735		D12P	18.827	18.542	18.684
D03T2	21.287	24.303	22.745		E12P	19.240	18.792	19.015
D03T3	22.608	23.032	22.819		F12P	17.977	17.986	17.982
D04T1	21.946	24.040	22.969		A12L	18.219	18.908	18.561
D04T2	21.322	24.028	22.635		B12L	18.161	18.207	18.184
D04T3	22.131	22.597	22.363		C12L	18.234	18.538	18.386
D05T1	21.035	24.062	22.498		D12L	18.626	18.591	18.608
D05T2	21.808	23.958	22.857		E12L	18.567	18.722	18.644
D05T3	22.454	22.674	22.564		F12L	17.590	17.973	17.781
D06T1	21.137	23.337	22.210		B24C	17.560	17.933	17.746
D06T2	21.002	23.844	22.378		C24C	18.317	18.235	18.276
D06T3	23.220	23.646	23.432		D24C	18.665	18.926	18.795
D07T1	21.253	24.090	22.627		E24C	18.585	18.676	18.630
D07T2	21.322	23.819	22.536		F24C	17.557	17.750	17.653
D07T3	23.189	23.158	23.173		A24P	19.107	19.723	19.413
D08T1	21.041	23.544	22.257		B24P	18.412	17.972	18.191
D08T2	21.011	23.625	22.280		C24P	18.847	18.387	18.616
D08T3	23.114	23.556	23.334		D24P	19.529	19.364	19.446
D09T1	22.014	23.454	22.723		E24P	19.720	18.877	19.294
D09T2	21.870	23.233	22.541		F24P	18.051	17.896	17.974
D09T3	23.099	23.587	23.342		A24L	18.168	19.869	18.999
D10T1	22.712	24.052	23.373		B24L	18.053	18.093	18.073
D10T2	21.654	23.093	22.362		C24L	18.566	18.700	18.633
D10T3	23.622	23.974	23.797		D24L	18.940	19.508	19.222
D11T1	21.768	24.224	22.963		E24L	18.761	18.741	18.751
D11T2	22.253	23.420	22.829		F24L	17.279	17.638	17.458
D11T3	23.336	23.100	23.218		A48C	18.575	19.489	19.027
D12T1	22.436	24.033	23.221		B48C	18.281	18.526	18.403
D12T2	22.756	24.191	23.462		C48C	18.036	18.236	18.136
D12T3	23.598	23.238	23.417		D48C	18.572	18.693	18.632

D13T1	22.874	23.961	23.411		E48C	18.323	18.776	18.548
D13T2	22.775	23.276	23.024		F48C	17.145	17.912	17.524
D13T3	23.583	23.253	23.417		A48P	19.428	19.883	19.654
D14T1	21.966	23.349	22.647		B48P	18.946	18.642	18.793
D14T2	23.153	21.796	22.464		C48P	18.958	18.532	18.743
D14T3	23.961	23.541	23.750		D48P	19.387	18.995	19.190
D15T1	22.750	23.929	23.332		E48P	19.019	18.884	18.951
D15T2	23.663	24.308	23.983		F48P	18.627	18.795	18.711
D15T3	23.867	23.415	23.640		A48L	19.382	20.463	19.915
D16T1	24.072	24.384	24.228		B48L	18.091	18.271	18.181
D16T2	22.960	21.637	22.289		C48L	18.163	18.266	18.215
D16T3	23.285	22.512	22.895		D48L	18.804	18.789	18.797
D17T1	23.766	24.520	24.140		E48L	18.282	18.567	18.424
D17T2	22.375	22.787	22.580		F48L	17.750	18.521	18.131
D17T3	23.783	22.870	23.322		A72C	18.061	19.006	18.528
					B72C	18.008	18.264	18.136
					C72C	18.105	18.882	18.489
					D72C	18.423	18.748	18.585
					E72C	17.967	18.536	18.249
					F72C	17.395	18.292	17.838
					A72P	19.072	20.041	19.551
					B72P	18.711	18.600	18.656
					C72P	19.489	19.496	19.492
					D72P	17.925	17.885	17.905
					E72P	19.190	19.105	19.147
					F72P	18.660	18.995	18.827
					A72L	18.627	19.268	18.945
					B72L	18.562	18.518	18.540
					C72L	18.732	18.999	18.865
					D72L	18.779	18.572	18.676
					E72L	18.767	18.786	18.776
					F72L	17.813	18.189	18.000

[1] Ct values determined by Applied Biosystems 7500 Fast software; representing average of technical triplicate reactions per sample. Experimental transcript expression was normalized against the geometric mean of the two normalizers.

[2] Early embryonic / larval samples: D00-D17 represents 0 days post-fertilization to 17 days post-fertilization. T=tank (replicate) number.

[3] Macrophage samples: A-F represents individual fish. 12, 24, 48, 72 = time (h) post stimulation. C = control (PBS); P = poly(I:C); L = LPS.